Sensor and Simulation Notes

Note 201

September 1974

Modes on a Finite-Width, Parallel-Plate Simulator
I.   Narrow Plates

Lennart Marin
Dikewood Corporation, Westwood Research Branch
Los Angeles, California

Abstract

The higher-order TE and TM modes on a simulator consisting of
two, parallel, narrow plates are studied. Expressions for the com-
plex transverse propagation constants are found showing that the
TM modes are less damped as they propagate along the line than are
the TE modes. The transverse variation of both the longitudinal
and the transverse field components of the lowest TM modes are
mapped. A general integral equation is also derived which is suit-
able for the numerical evaluation of the leaky modes on a parallel-
plate simulator having an arbitrary separation-to-width ratio of the
parallel plates.

Contents

Illustrations

4

I. Introduction

Many EMP simulators, such as the ATLAS I and II, the ARES and the ALECS, make use of a parallel-plate transmission line as a guiding structure for the electromagnetic field (see Fig. 1). One reason for using parallel-plate simulators is that they support a TEM mode. In many of these simulators the field distribution of the TEM mode is nearly uniform over a significant portion of their cross section. For this reason and the reason that the TEM mode propagates with the speed of light, the TEM mode provides a good approximation to the free-space nuclear EMP. The TEM mode propagates at all frequencies but for frequencies such that the free-space wavelength is of the same order as the cross-sectional dimensions of the simulator the TEM mode alone may not be the dominant part of the simulator field. In most cases it is desirable to launch fast rising pulses on the parallel-plate simulators whose risetimes are significantly smaller than the transit time across the simulator. In doing so the simulator field will consist not only of the TEM mode but also of higher order modes and a continuous spectrum.

The properties of the TEM mode on two parallel plates have been investigated using conformal mapping techniques[1-6]. The effect of replacing the parallel plates by a number of parallel wires has also been investigated[1,7]. The transient currents on a simulator consisting of two parallel wires where each wire is fed by a slice-generator with a step-function voltage has been studied in [8]. It is found in [8] that when the two wires are fed in a push-pull manner, the transient induced current can be expressed in terms of an infinite sum plus an infinite integral. One term in the sum represents the contribution from the TEM mode, whereas the other terms can be interpreted as the contribution from higher order modes, the properties of which will be discussed below. The combined contribution from all modes represent the contribution from the discrete part of the spectrum, whereas the integral represents the contribution from the continuous part of the spectrum.

The discrete spectrum of an open waveguide has properties which are different from those of the discrete spectrum of a closed waveguide. In regions of finite extent bounded by impenetrable walls, i.e., closed regions, the modes (which are the source-free solutions of the Maxwell equations) generally possess orthogonality and completeness properties such that an arbitrary field distribution

5
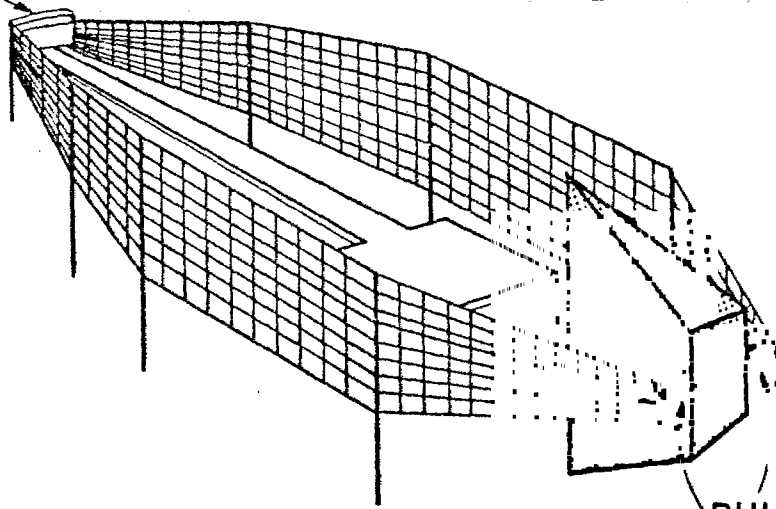
TERMINATION

PULSERS

TERMINATION
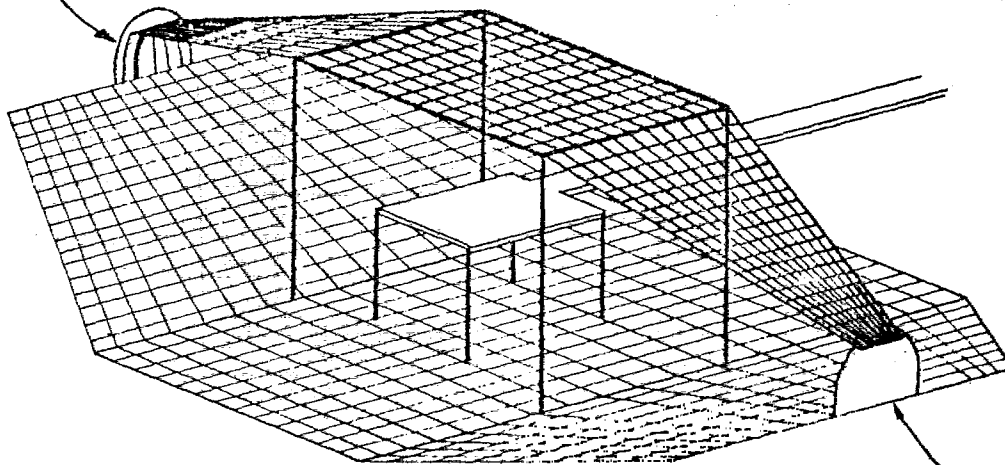
PULSER

Figure 1. Schematic picture of ATLAS I and II simulators.

can be represented by their superposition. These modes are square integrable over the cross section of the waveguide (because they have finite energy), satisfy the source-free Maxwell equations and the appropriate boundary conditions on the walls of the waveguide. In regions of infinite extent, i.e., open regions, there may exist a corresponding discrete spectrum. However, to get a complete representation of the field these modes must in general be supplemented by a continuous spectrum. All modes of the discrete spectrum satisfy the source-free field equations and the boundary conditions on the surface of the waveguide. In contradistinction to the modes on a closed waveguide many modes of the discrete spectrum of an open waveguide are not square integrable on the cross section of the waveguide. In fact, the field components of these modes or more aptly the leaky modes grow exponentially in the transverse direction far away from the waveguide. Mathematically, this fact can be stated as follows: the propagation constants of the leaky modes belong to the Riemann sheet in which the radiation condition is violated. Although these modes in general do not form a complete set of orthogonal functions, they can nevertheless be employed to obtain convergent representations of the field in certain regions in space, for example, the region between the two parallel plates in a parallel-plate simulator.

Some comments are now in order concerning a method that may be used when determining the excitation coefficient of each leaky mode. The "ordinary" technique of matching fields at a cross section of a waveguide, which is so useful when determining the excitation coefficient of each mode in a closed waveguide, does not necessarily apply to open waveguides, since the leaky modes are neither square integrable nor do they form a complete set of functions. Instead of matching fields at a cross section of a waveguide the excitation coefficients of the leaky modes can be obtained by requiring that the total field satisfies the boundary conditions on the waveguide walls (c.f. [8]).

Finally, we mention that the leaky modes are the nontrivial solutions of the Maxwell equations in two dimensional regions which are exterior to a region of finite extent. Therefore, the leaky modes in two dimensions are the counterparts to the natural modes[9] in three dimensions.

This note is a continuation of a previous note[8] which treats the transient field around two parallel wires excited at a delta gap. Whereas the attention was focused on the time history of the induced currents on the wires in [8]

7

this note places more emphasis on the field distribution of certain leaky modes on two narrow parallel plates. These modes are found by formulating two different scalar integral equations of the first kind for the longitudinal components of the electric and magnetic fields, respectively. When the separation between the plates is large compared to their width these integral equations can be solved analytically by first transforming them into a Fredholm integral equation of the second kind which in turn can be solved using perturbation techniques. The results of the field calculations are presented in graphical forms for the transverse components of the electric and magnetic fields of the two lowest TM modes. Graphical results are given of the magnitude of the electric field of the three lowest TM modes and of the transverse propagation constant.

A general method of reducing scalar scattering from open surfaces to the solution of Fredholm integral equations of the second kind is given in the Appendix. Both the Dirichlet problem and the Neumann problem are discussed. These integral equations are then used to derive suitable integral equations of the second kind for the TE fields and the TM fields on two parallel plates of finite width. Certain properties of the integral equations are derived. It is also shown how they can be used to numerically determine the transverse, complex propagation constant and field distribution of the leaky modes on two parallel plates of arbitrary separation-to-width ratio. Due to the complexity of these numerical calculations they are left to a future note.

II. Integral Equations for the Field

Consider a waveguide that consists of two parallel plates of finite width, the width of each plate being $2w$ and the distance separating the two plates being $2h$, (see Fig. 2). The waveguide is excited by an incident electromagnetic field $\underline{\mathcal{E}}^{inc}(\underline{r},t)$, $\underline{\mathcal{K}}^{inc}(\underline{r},t)$. To find the scattered field $\underline{\mathcal{E}}(\underline{r},t)$, $\underline{\mathcal{K}}(\underline{r},t)$ Laplace transform methods will be used,

$$\underline{E}(x,y,\zeta,s) = \int_{-\infty}^{\infty}\int_{-\infty}^{\infty} \underline{\mathcal{E}}(\underline{r},t)\exp(-\zeta z)\exp(-st)dzdt \qquad (1)$$

and similarly for the magnetic field. The coordinate system is so chosen that the z-axis is directed along the axis of the waveguide and that the x and y axes span the plane which is perpendicular to the axis of the waveguide (see Fig. 2). The transverse field components in the Laplace transform domain are related to the longitudinal components in that domain via

$$\underline{E}_t(x,y,\zeta,s) = -\zeta p^{-2}\nabla_t E_z(x,y,\zeta,s) - s\mu_o p^{-2}\hat{z}\times\nabla_t H_z(x,y,\zeta,s)$$

$$(2)$$

$$\underline{H}_t(x,y,\zeta,s) = -\zeta p^{-2}\nabla_t H_z(x,y,\zeta,s) + s\varepsilon_o p^{-2}\hat{z}\times\nabla_t E_z(x,y,\zeta,s)$$

where $p = \sqrt{s^2 c^{-2} - \zeta^2}$, c is the vacuum speed of light and the index t denotes the transverse field components. Thus, once the longitudinal components of both the electric and magnetic fields are determined in the Laplace transform domain, the scattered field $\underline{\mathcal{E}}(\underline{r},t)$ is given by (2) and the inverse Laplace transform integral

$$\underline{\mathcal{E}}(\underline{r},t) = \frac{1}{2\pi i}\int_{C_s}\left[\frac{1}{2\pi i}\int_{C_\zeta}\underline{E}(x,y,\zeta,s)\exp(\zeta z)d\zeta\right]\exp(st)ds \qquad (3)$$

where C_s and C_ζ are paths of integration parallel to the imaginary axes in the complex s and ζ planes. The scattered magnetic field $\underline{\mathcal{K}}(\underline{r},t)$ is determined using a similar procedure.

From the Maxwell equations it follows that both E_z and H_z satisfy the two-dimensional Helmholtz equation,

9
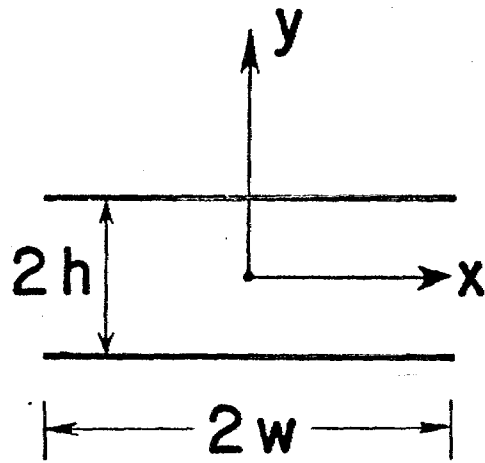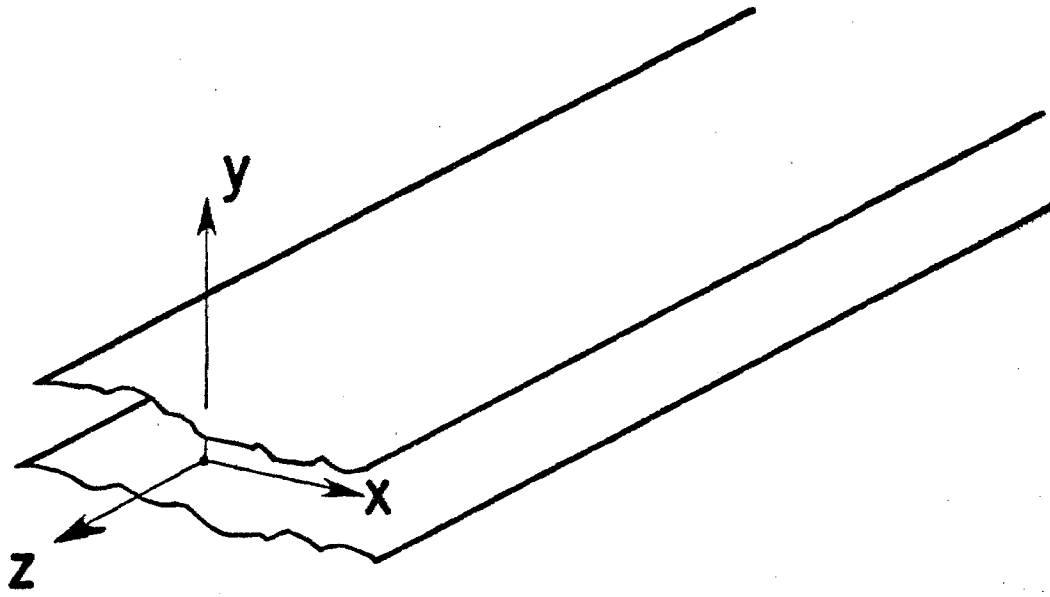
Figure 2. Two, finite-width, parallel plates.

$$\nabla_t^2 E_z - p^2 E_z = 0, \qquad \nabla_t^2 H_z - p^2 H_z = 0 \qquad (4)$$

and the boundary conditions on the plates imply that

$$E_z + E_z^{inc} = 0, \qquad \text{on } S_+ \text{ and } S_-$$

$$(5)$$

$$\frac{\partial H_z}{\partial y} + \frac{p^2}{s\mu_o} E_x^{inc} - \frac{\zeta}{s\mu_o} \frac{\partial E_z^{inc}}{\partial x} = 0 \qquad \text{on } S_+ \text{ and } S_-$$

where S_+ (S_-) denotes the cross-section of the upper (lower) plate, i.e., in mathematical terms $S_\pm = \{x,y: |x| < w, \ y = \pm h\}$. One observes that E_z (H_z) is given by the solution of a Dirichlet (Neumann) boundary-value problem.

Next, integral equations will be formulated the solutions of which enable one to determine E_z and H_z. Therefore, first note that E_z and $(\partial/\partial y)H_z$ are continuous everywhere (including on $S_\pm$). However, $(\partial/\partial y)E_z$ and H_z can be discontinuous across $S_\pm$ and so the following quantities are introduced

$$f_\pm(x) = \lim_{\varepsilon \to 0} \left[\frac{\partial E_z}{\partial y}(x, \pm h + \varepsilon, \zeta, s) - \frac{\partial E_z}{\partial y}(x, \pm h - \varepsilon, \zeta, s) \right]$$

$$(6)$$

$$(s\mu_o)^{-1} g_\pm(x) = \lim_{\varepsilon \to 0} \left[H_z(x, \pm h + \varepsilon, \zeta, s) - H_z(x, \pm h - \varepsilon, \zeta, s) \right].$$

The paths of integration in (3) has to be chosen so that the scattered field satisfies the radiation condition at infinity. This implies that E_z and H_z satisfy the radiation condition as $(x^2 + y^2)^{\frac{1}{2}}$ tends to infinity. Keeping this in mind the Green's theorem gives

$$E_z(x,y,\zeta,s) = \int_{-w}^{w} G(x,y,x',h;p) f_+(x')dx' + \int_{-w}^{w} G(x,y,x',-h;p) f_-(x')dx'$$

$$(7)$$

$$s\mu_o H_z(x,y,\zeta,s) = -\int_{-w}^{w} \frac{\partial G}{\partial y'}(x,y,x',h;p) g_+(x')dx' - \int_{-w}^{w} \frac{\partial G}{\partial y'}(x,y,x',-h;p) g_-(x')dx'$$

where

$$G(x,y,x',y';p) = \frac{1}{2\pi} K_o\left(p\sqrt{(x-x')^2 + (y-y')^2}\right)$$

11

and $K_o(\xi)$ is the modified Bessel function of the first kind. Taking the y-derivative of the latter of the equations in (6) and using the fact that the Green's function satisfies the differential equation

$$\nabla_t^2 G - p^2 G = 0, \qquad x \neq x' \quad \text{and} \quad y \neq y' \tag{8}$$

one gets the following expression

$$s\mu_o \frac{\partial H_z}{\partial y}(x,y,\zeta,s) = -\left(\frac{\partial^2}{\partial x^2} - p^2\right)\left[\int_{-w}^{w} G(x,y,x',h;p)g_+(x')dx'\right.$$
$$\left. + \int_{-w}^{w} G(x,y,x',-h;p)g_-(x')dx'\right]. \tag{9}$$

By requiring that the total longitudinal electric field vanishes on the plates one obtains the following set of integral equations for $f_\pm(x)$

$$\int_{-w}^{w} G(x,h,x',h;p)f_+(x')dx' + \int_{-w}^{w} G(x,h,x',-h;p)f_-(x')dx' = \alpha_+(x), \qquad |x| < w \tag{10}$$

$$\int_{-w}^{w} G(x,-h,x',h;p)f_+(x')dx' + \int_{-w}^{w} G(x,-h,x',-h;p)f_-(x')dx' = \alpha_-(x), \qquad |x| < w$$

where

$$\alpha_\pm(x) = -E_z^{inc}(x,\pm h,\zeta,s).$$

Similarly, the boundary conditions (5) for $(\partial/\partial y)H_z$ on the plates result in the following differential-integral equations for $g_\pm(x)$

$$\left(\frac{d^2}{dx^2} - p^2\right)\left[\int_{-w}^{w} G(x,h,x',h;p)g_+(x')dx' + \int_{-w}^{w} G(x,h,x',-h;p)g_-(x')dx'\right] = \beta_+(x),$$
$$|x| < w$$
$$\tag{11}$$

$$\left(\frac{d^2}{dx^2} - p^2\right)\left[\int_{-w}^{w} G(x,-h,x',h;p)g_+(x')dx' + \int_{-w}^{w} G(x,-h,x',-h;p)g_-(x')dx'\right] = \beta_-(x),$$
$$|x| < w$$

where

$$\beta_{\pm}(x) = p^2 E_x^{inc}(x, \pm h, \zeta, s) - \zeta \frac{\partial E_y^{inc}}{\partial y}(x, \pm h, \zeta, s).$$

This set of differential integral equations can be integrated to yield the following set of integral equations

$$\int_{-w}^{w} G(x, h, x', h; p) g_+(x') dx' + \int_{-w}^{w} G(x, h, x', -h; p) g_-(x') dx'$$

$$= A_+ \cosh(px) + B_+ \sinh(px) + \int_{-w}^{w} \frac{\sinh(p|x-x'|)}{2p} \beta_+(x') dx'$$

(12)

$$\int_{-w}^{w} G(x, -h, x', h; p) g_+(x') dx' + \int_{-w}^{w} G(x, -h, x', -h; p) g_-(x') dx'$$

$$= A_- \cosh(px) + B_- \sinh(px) + \int_{-w}^{w} \frac{\sinh(p|x-x'|)}{2p} \beta_-(x') dx'$$

where $A_{\pm}$ and $B_{\pm}$ are constants of integration to be determined from the edge conditions which require that

$$g_{\pm}(x) \sim (w^2 - x^2)^{\frac{1}{2}} \qquad \text{as} \quad x \to \pm w.$$

The integral equations (10) and (12) constitute the mathematical formulation of the scattering problem. In the next section the two sets of integral equations (10) and (12) will be solved for narrow plates, i.e., when $w \ll h$.

III. Solution of the Integral Equations in the Case of Narrow Plates

When the width of the plates is small compared to the distance separating the two plates an approximate solution of the sets of integral equations (10) and (12) can be found using analytical techniques. In the first part of this section a solution of (10) will be obtained from which all the properties of the TM field (E waves) can be determined. Then, (12) will be solved for the TE field (H waves).

A. The Transverse Magnetic Field

The set of two coupled integral equations (10) can be transformed into two uncoupled integral equations in the following way: first introduce the two functions $u_{\pm}(x) = f_{+}(x) \pm f_{-}(x)$, so that $2f_{\pm}(x) = u_{+}(x) \pm u_{-}(x)$ and then substitute them into (10). By adding and subtracting the two equations in (10) one arrives at the following two uncoupled integral equations

$$\int_{-w}^{w} G(x,h,x',h;p)u_{\pm}(x')dx' \pm \int_{-w}^{w} G(x,h,x',-h;p)u_{\pm}(x')dx' = \mu_{\pm}(x) \qquad (13)$$

where $\mu_{\pm}(x) = \alpha_{+}(x) \pm \alpha_{-}(x)$. The solution u_{+} corresponds to the case where the longitudinal current on one plate has the same magnitude and direction as that on the other plate, whereas the solution u_{-} corresponds to the case where the longitudinal current on one plate has the same magnitude but opposite direction as that on the other plate. The terms "push-push" and "push-pull" were used in [8] for these two cases.

Now, consider the case where $w \ll h$. In this case there exists a complex p such that $|pw| \ll 1$ but $|ph|$ is not necessarily small. With this restriction on p one can approximate the kernels in (13) by the following expressions

$$G(x,h,x',h;p) \approx (2\pi)^{-1}\{-\gamma - \ln(p|x-x'|/2) + p^2(x-x')^2/4[1 - \gamma - \ln(p|x-x'|/2)]\}$$

$$(14)$$

$$G(x,h,x',-h;p) \approx (2\pi)^{-1}[K_o(2ph) - (x-x')^2 p/(2h)K_1(2ph)]$$

14

where γ is Euler's constant, $\gamma \approx 0.5772\ldots$ Using these approximate expressions for the kernels in (13) one arrives at the following approximate integral equations for $u_\pm$,

$$\int_{-w}^{w} \ln(p|x-x'|)u_\pm(x')dx' - \int_{-w}^{w} [\ln 2 - \gamma \pm K_o(2ph)]u_\pm(x')dx'$$

$$+ \int_{-w}^{w} L_\pm(x,x')u_\pm(x')dx' = -2\pi\mu_\pm(x) \qquad (15)$$

where

$$L_\pm(x,x') = p^2(x-x')^2[\ln(p|x-x'|) - \ln 2 + \gamma \pm (2/ph)K_1(2ph)]/4.$$

The integral equation (15) where the kernel has a logarithmic singularity at $x = x'$ can be transformed into the following Fredholm integral equation of the second kind with the aid of the Cauchy integral[10]

$$u_\pm(x) + \frac{\ln(2/pw)-\gamma\pm K_o(2ph)}{\pi \ln 2 \sqrt{w^2-x^2}} \int_{-w}^{w} u_\pm(x')dx'$$

$$- \frac{w}{\pi^2 \ln 2 \sqrt{w^2-x^2}} \int_{-w}^{w}\int_{-w}^{w} \frac{L_\pm(x',x'')u_\pm(x'')}{\sqrt{w^2-x'^2}} dx'dx''$$

$$+ \frac{w}{\pi^2 \sqrt{w^2-x^2}} \int_{-w}^{w} \frac{\sqrt{w^2-x'^2}}{x'-x} \left[\frac{d}{dx'}\int_{-w}^{w} L_\pm(x',x'')u_\pm(x'')dx''\right]dx'$$

$$= \frac{2w}{\pi \ln 2 \sqrt{w^2-x^2}} \int_{-w}^{w} \frac{\mu_\pm(x')}{\sqrt{w^2-x'^2}} dx' - \frac{2w}{\pi\sqrt{w^2-x^2}} \fint_{-w}^{w} \frac{\mu_\pm'(x')\sqrt{w^2-x'^2}}{x'-x} dx' \qquad (16)$$

where $\fint$ denotes the principal-value integral.

The integral equation (16) can be solved iteratively by making the following observation: when $|pw| \ll 1$ the norm of the kernel $L_\pm(x,x')$ is small, so that the contribution from the last two terms on the left-hand side of (16) is small compared to the contribution from the first two terms. Thus,

15

to the first approximation one has $u_\pm \approx u_\pm^o$ where $u_\pm^o$ satisfies the integral equation

$$u_\pm^o(x) + \frac{\ln(2/pw)-\gamma \pm K_o(2ph)}{\pi \ln 2 \sqrt{w^2-x^2}} \int_{-w}^{w} u_\pm^o(x')dx'$$

$$= \frac{2w}{\pi \ln 2\sqrt{w^2-x^2}} \int_{-w}^{w} \frac{\mu_\pm(x')}{\sqrt{w^2-x'^2}}dx' - \frac{2w}{\pi\sqrt{w^2-x^2}} \int_{-w}^{w} \frac{\mu_\pm'(x')\sqrt{w^2-x'^2}}{x'-x}dx'. \quad (17)$$

A closed-form solution of this integral equation is found to be

$$u_\pm^o(x) = \frac{2w}{\pi[\ln(4/pw)-\gamma \pm K_o(2ph)]} \frac{1}{\sqrt{w^2-x^2}} \int_{-w}^{w} \frac{\mu_\pm(x')}{\sqrt{w^2-x'^2}}dx'$$

$$- \frac{2w}{\pi\sqrt{w^2-x^2}} \int_{-w}^{w} \frac{\mu_\pm'(x')\sqrt{w^2-x'^2}}{x'-x}dx'. \quad (18)$$

To find a better approximation for $u_\pm$ one writes

$$u_\pm = u_\pm^o + u_\pm^1 \quad (19)$$

where $\|u_\pm^1\| << \|u_\pm^o\|$. Substituting the expression (19) into (16) and taking into account the facts that the norm of $L_\pm(x,x')$ is small and that $u_\pm^o$ satisfies (17) the following expression for $u_\pm^1$ is obtained,

$$u_\pm^1(x) = \frac{w}{\pi^2[\ln(4/pw)-\gamma \pm K_o(2ph)]} \frac{1}{\sqrt{w^2-x^2}} \int_{-w}^{w}\int_{-w}^{w} \frac{L_\pm(x',x'')u_\pm^o(x'')}{\sqrt{w^2-x'^2}}dx'dx''$$

$$- \frac{w}{\pi^2\sqrt{w^2-x^2}} \int_{-w}^{w} \frac{\sqrt{w^2-x'^2}}{x'-x}\left[\frac{d}{dx'}\int_{-w}^{w}L_\pm(x',x'')u_\pm^o(x'')dx''\right]dx'. \quad (20)$$

The analytical properties in the complex p-plane of the solutions (18) and (20) will now be investigated. When the incident field is a holomorphic function of p it follows immediately from (20) that $u_\pm$ has two types of singularities: a branch-point at $p = 0$ and poles at those values of p for

16

which the homogeneous integral equation (16) has a nontrivial solution. Each one of these poles corresponds to a mode and in the next section certain properties of these modes will be investigated. It should also be pointed out that although these analytical properties in the p-plane of the scattered field has only been proven for narrow plates, they are shared by the scattered field on a parallel plate waveguide of arbitrary width-to-separation ratio.

B. The Transverse Electric Field

The transverse electric field is determined from the solution of the set of integral equations (12). Similarly to the TM case one introduces the functions $v_{\pm}(x) = g_+(x) \pm g_-(x)$, so that $2g_{\pm}(x) = v_+(x) \pm v_-(x)$ and $v_{\pm}(x)$ satisfies the integral equation

$$\int_{-w}^{w} G(x,h,x',h;p)v_{\pm}(x')dx' \pm \int_{-w}^{w} G(x,h,x',-h;p)v_{\pm}(x')dx'$$

$$= C_{\pm} \cosh(px) + D_{\pm} \sinh(px) + \nu_{\pm}(x) \qquad (21)$$

where

$$\nu_{\pm}(x) = \int_{-w}^{w} (2p)^{-1} \sinh(p|x-x'|)[\beta_+(x') \pm \beta_-(x')]dx'$$

$$C_{\pm} = A_+ \pm A_-, \qquad D_{\pm} = B_+ \pm B_-$$

and the constants $C_{\pm}$ and $D_{\pm}$ are determined from the edge conditions at $x = \pm w$. By comparing (16) and (21) it follows from (13), (18), (19), (20) that one has the following approximate solution of (21),

$$v_{\pm}(x) \approx v_{\pm}^{o}(x) + v_{\pm}^{1}(x) \qquad (22)$$

where

$$v_{\pm}^{o}(x) = \frac{2w}{\pi[\ln(4/pw)-\gamma\pm K_o(2ph)]} \frac{1}{\sqrt{w^2-x^2}} \int_{-w}^{w} \frac{C_{\pm}\cosh(px')+D_{\pm}\sinh(px') + \nu_{\pm}(x')}{\sqrt{w^2-x'^2}} dx'$$

$$- \frac{2w}{\pi\sqrt{w^2-x^2}} \int_{-w}^{w} \frac{[pC_{\pm}\sinh(px')+pD_{\pm}\cosh(px')+\nu_{\pm}'(x')]\sqrt{w^2-x'^2}}{x'-x} dx' \qquad (23)$$

17

$$v_{\pm}^{1}(x) = \frac{w}{\pi^2[\ln(4/pw)-\gamma\pm K_o(2ph)]} \frac{1}{\sqrt{w^2-x^2}} \int_{-w}^{w}\int_{-w}^{w} \frac{L_{\pm}(x',x'')v_{\pm}^{o}(x'')}{\sqrt{w^2-x'^2}} dx'dx''$$

$$- \frac{w}{\pi^2\sqrt{w^2-x^2}} \int_{-w}^{w} \frac{\sqrt{w^2-x'^2}}{x'-x}\left[\frac{d}{dx'}\int_{-w}^{w} L_{\pm}(x',x'')v_{\pm}^{o}(v'')dx''\right]dx'. \tag{24}$$

To determine the unknown constants $C_{\pm}$ and $D_{\pm}$ one invokes the edge conditions at $x = \pm w$ which require that $v_{\pm}(x) \sim (w^2 - x^2)^{\frac{1}{2}}$ as $x \to \pm w$. These conditions result in the following equations

$$\frac{1}{\ln(4/pw)-\gamma\pm K_o(2ph)} \int_{-w}^{w} \frac{C_{+}\cosh(px')+ D_{\pm}\sinh(px')+v_{\pm}(x')}{\sqrt{w^2-x'^2}} dx'$$

$$= -\int_{-w}^{w}[pC_{\pm}\sinh(px') + pD_{\pm}\cosh(px') + v_{\pm}'(x')]\sqrt{\frac{a+x'}{a-x'}} dx'$$

$$= \int_{-w}^{w}[pC_{\pm}\sinh(px') + pD_{\pm}\cosh(px') + v_{\pm}'(x')]\sqrt{\frac{a-x'}{a+x'}} dx' \tag{25}$$

from which one gets

$$C_{\pm} = \frac{-1}{\pi[I_o(pw)+pwI_1(pw)F_{\pm}(p,w,h)]} \int_{-w}^{w} \frac{v_{\pm}(x')+F_{\pm}(p,w,h)x'v_{\pm}'(x')}{\sqrt{w^2-x'^2}} dx'$$

$$\tag{26}$$

$$D_{\pm} = \frac{-1}{\pi pa I_o(pa)} \int_{-w}^{w} \frac{av_{\pm}'(x')}{\sqrt{w^2-x'^2}} dx'$$

where

$$F_{\pm}(p,w,h) = \ln(4/pw) - \gamma \pm K_o(2ph)$$

and $I_n(\xi)$ is the modified Bessel function of the first kind.

18

Again, it is noted that $v_{\pm}(x)$ has a branch point at the origin of the p-plane besides poles for certain values of p. In the next section it will be shown that there are no poles, however, for $|pw| \ll 1$.

IV. Modes on Narrow Plates

In the previous section it was pointed out that the scattered field has two types of singularities in the complex p-plane, namely, a branch point at $p = 0$ and poles. When evaluating the inverse Laplace transform integral (3) the branch point shows up in the form of an integral around the corresponding branch cut and the poles give rise to modes propagating along the waveguide[8]. The z-dependence of these modes is given by $\exp[-z(s^2 c^{-2} - p_n^2)^{1/2}]$ where p_n has the value such that the homogeneous equations (10) or (12) have a non-trivial solution. The quantity p_n may be called the transverse propagation constant of the mode and is equal to the imaginary unit times the transverse wavenumber. To each mode one associates a field distribution. Later in this section the transverse electric and magnetic fields of certain important TM modes will be investigatied. First, the transverse propagation constants for both TM and TE modes will be obtained.

A. Transverse Propagation Constants of TM Modes

The transverse propagation constants of the TM modes are given by the poles in $u_\pm(x)$, i.e., by those values of p for which the homogeneous integral equation (13) has a nontrivial solution. Using the perturbation method employed in Sec. III an approximate value of p is given by the nontrivial solution of

$$\hat{u}_\pm^o(x) + \frac{\ln(2/pw) - \gamma \pm K_o(2ph)}{\pi \ln 2 \sqrt{w^2 - x^2}} \int_{-w}^{w} \hat{u}_\pm^o(x')dx' = 0 \tag{27}$$

which, after integration, yields

$$[\ln(4/pw) - \gamma \pm K_o(2ph)] \int_{-w}^{w} \hat{u}_\pm^o(x)dx = 0. \tag{28}$$

From (27) one notes that $\hat{u}_\pm^o(x)$ is an even function of the form $\hat{u}_\pm^o(x) = A/(w^2 - x^2)^{-1/2}$. Thus, from (27) and (28) it is clear that $A \neq 0$ only when

$$\ln(4/pw) - \gamma \pm K_o(2ph) \approx 0. \tag{29}$$

The determinental equation (29) for TM modes on two parallel, narrow plates

20

can be compared with that for two parallel wires with radii a and separated by a distance $2h$. In the wire case the determinental equation is[8].

$$\ln(2/pa) - \gamma \pm K_o(2ph) = 0 \tag{30}$$

and the factor of 2 difference in the logarithmic term between the two expressions can be accounted for by noting that the effective radius of the strip is $w/2$, i.e., a strip of width $2w$ has the same capacitance per unit length as a cylinder with radius $w/2$.

The transcendental equation (29) has to be solved numerically, and its solutions are denoted by $p_{on}^{\pm}$. The corresponding nontrivial solution of $\hat{u}_{\pm}^{o}$ is then

$$\hat{u}_{\pm}^{o}(x) = \frac{w}{\pi\sqrt{w^2-x^2}} \tag{31}$$

and $\hat{u}_{\pm}^{o}(x)$ is normalized so that

$$\int_{-w}^{w} \hat{u}_{\pm}^{o}(x)dx = 1. \tag{32}$$

Note that this function is independent of $p_{on}^{\pm}$.

To get a more accurate value of the poles of $u_{\pm}(x)$ in (16) one substitutes the expansions

$$p_n^{\pm} = p_{on}^{\pm} + p_{1n}^{\pm}, \qquad |p_{1n}^{\pm}| << |p_{on}^{\pm}|$$

$$\tag{33}$$

$$u_{\pm} = \hat{u}_{\pm}^{o} + \hat{u}_{\pm}^{1}, \qquad \|\hat{u}_{\pm}^{1}\| << \|\hat{u}_{\pm}^{o}\|$$

into the homogeneous equation (16) and obtains the following equation

$$\hat{u}_{\pm}^{1}(x) - \frac{1}{\pi\sqrt{w^2-x^2}} \int_{-w}^{w} \hat{u}_{\pm}^{1}(x')dx' = \frac{wp_{1n}^{\pm} \pm 2whp_{on}^{\pm}p_{1n}^{\pm}K_1(2p_{on}^{\pm}h)}{p_{on}^{\pm}\pi \ln 2 \sqrt{w^2-x^2}} - \Delta_{\pm}(x) \tag{34}$$

21

where

$$\Delta_{\pm}(x) = \frac{-w}{\pi^3 \ln 2 \sqrt{w^2-x^2}} \int_{-w}^{w}\int_{-w}^{w} \frac{L_{\pm}(x',x'')}{\sqrt{(w^2-x'^2)(w^2-x''^2)}} \, dx'dx''$$

$$+ \frac{w}{\pi^3 \sqrt{w^2-x^2}} \int_{-w}^{w} \frac{\sqrt{w^2-x'^2}}{x'-x} \left[\frac{d}{dx'} \int_{-w}^{w} \frac{L_{\pm}(x',x'')}{\sqrt{w^2-x''^2}} \, dx'' \right] dx' .$$

By integrating (34) and using the fact that $u_{\pm}^1(x)$ is an even function not identically equal to zero the following expression for $p_{1n}^{\pm}$ is derived,

$$p_{1n}^{\pm} = \frac{(p_{on}^{\pm})^3 w^2 \{\pi^2+2-1.5\pi^2 \ln 2-(\pi^2-8)\gamma/4+(\pi^2-8)[\ln(wp_{on}^{\pm}/2)\pm 2(hp_{on}^{\pm})^{-1}K_1(2hp_{on}^{\pm})]/4\}}{\pi[1\pm 2hp_{on}^{\pm}K_1(2hp_{on}^{\pm})]} . \tag{35}$$

Equation (29) was solved numerically for the twelve lowest roots. These values were then used to numerically evaluate $p_{1n}^{\pm}$ from (35). The results of these calculations are shown in Fig. 3 and Table 1 where the normalized quantity $p_n^{\pm}w = (p_{on}^{\pm} + p_{1n}^{\pm})w$ is presented.

B. Transverse Propagation Constants of TE Modes

The transverse propagation constant for the TE modes are given by those values of p for which the homogeneous integral equation (21) has a nontrivial solution. Since the main concern of this note is the case where $|pw| << 1$ one can, in the first approximation, neglect the second term on the left-hand side of (23) and also makes the approximations $\cosh(px) \approx 1$, $\sinh(px) \approx px$. Thus, one has the following approximate homogeneous integral equation

$$v_{\pm}(x) + \frac{\ln(2/pw)-\gamma\pm K_0(2ph)}{\pi \ln 2 \sqrt{w^2-x^2}} \int_{-w}^{w} v_{\pm}(x')dx'$$

$$= \frac{2wC_{\pm}}{\ln 2 \sqrt{w^2-x^2}} + \frac{2wpD_{\pm}x}{\sqrt{w^2-x^2}} . \tag{36}$$
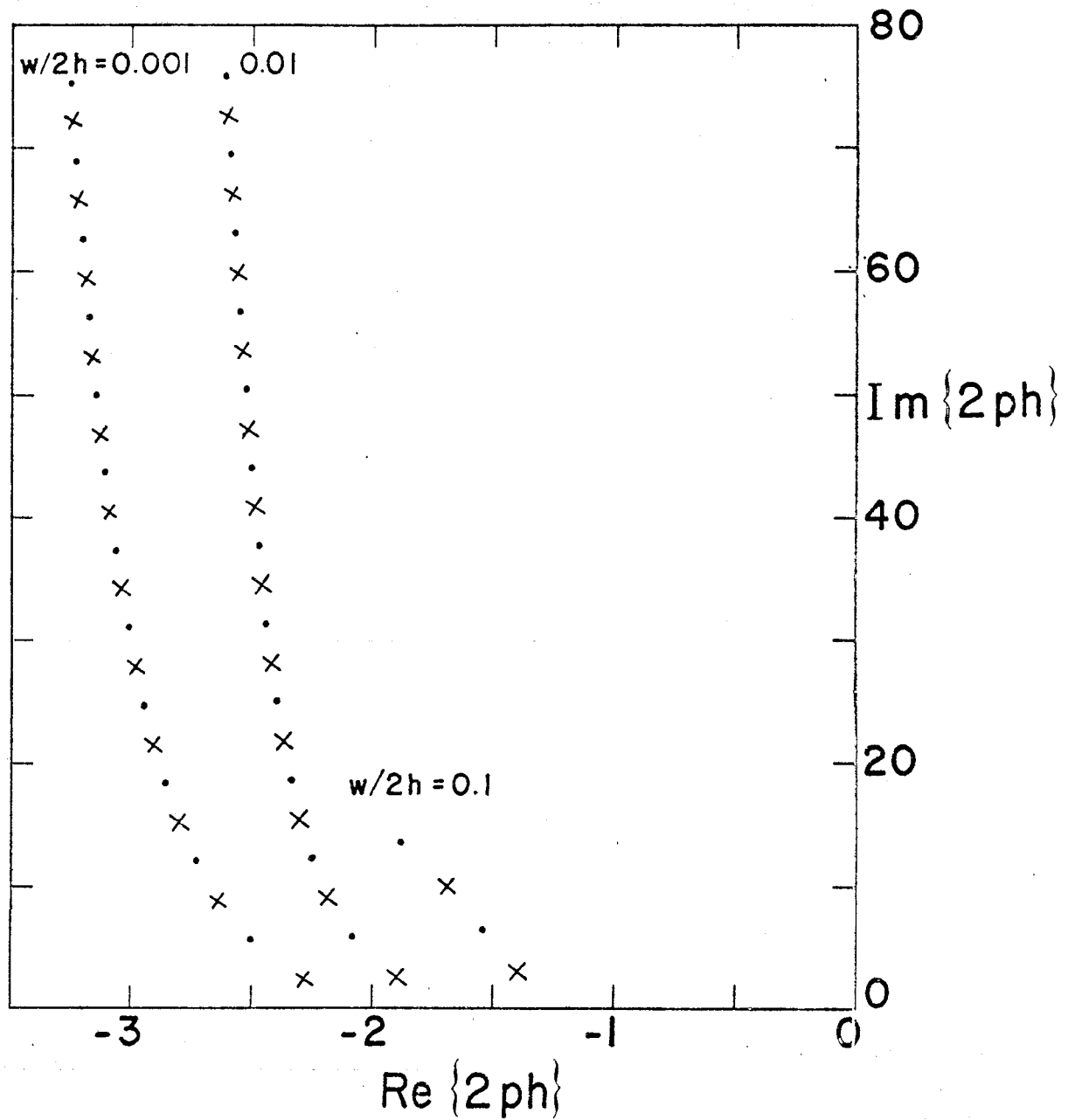
Figure 3. Transverse propagation constant of TM modes.

$w/2h$	n	$\text{Re}\{2p_n^+ h\}$	$\text{Im}\{2p_n^+ h\}$	$\text{Re}\{2p_n^- h\}$	$\text{Im}\{2p_n^- h\}$
0.01	1	−1.902	2.552	−2.084	5.836
	2	−2.185	9.051	−2.252	12.246
	3	−2.303	15.430	−2.342	18.611
	4	−2.374	21.785	−2.400	24.962
	5	−2.423	28.128	−2.443	31.305
	6	−2.461	34.464	−2.478	37.646
	7	−2.493	40.797	−2.506	43.959
	8	−2.519	47.126	−2.532	50.323
	9	−2.543	53.454	−2.555	56.662
	10	−2.566	59.780	−2.577	63.002
	11	−2.587	66.105	−2.598	69.342
	12	−2.608	72.429	−2.619	75.684
0.001	1	−2.280	2.349	−2.505	5.633
	2	−2.640	8.834	−2.734	12.011
	3	−2.805	15.178	−2.862	18.339
	4	−2.910	21.496	−2.951	24.652
	5	−2.986	27.805	−3.017	30.958
	6	−3.045	34.109	−3.070	37.260
	7	−3.093	40.410	−3.114	43.559
	8	−3.133	46.708	−3.151	49.857
	9	−3.167	53.005	−3.183	56.153
	10	−3.197	59.301	−3.211	62.448
	11	−3.224	65.596	−3.236	68.743
	12	−3.248	71.890	−3.259	75.037

Table 1.   The transverse propagation constant of the TM modes.

The first term on the right-hand side of (36) is an even function of x, whereas the second term is an odd function of x. From (36) one also observes that $v_\pm(x)$ can be represented as

$$v_\pm(x) = v_\pm^+(x) + v_\pm^-(x) \tag{37}$$

where $v_\pm^+(x)$ $(v_\pm^-(x))$ is an even (odd) function of x and that

$$v_\pm^+(x) + \frac{\ln(2/pw) - \gamma \pm K_0(2ph)}{\pi \ln 2 \sqrt{w^2 - w^2}} \int_{-w}^{w} v_\pm^+(x')dx' = \frac{2wC_\pm}{\ln 2 \sqrt{w^2 - x^2}}$$

$$v_\pm^-(x) = \frac{2wpD_\pm x}{\sqrt{w^2 - x^2}} \tag{38}$$

The edge conditions require that $v_\pm^\pm(x) \sim (w^2 - x^2)^{\frac{1}{2}}$ as $x \to \pm w$, and the only solutions of (38) satisfying the edge conditions are the trivial solutions $v_\pm^\pm(x) \equiv 0$, $C_\pm = 0$, $D_\pm = 0$. One therefore draws the conculusion that two narrow plates do not support a TE mode with a transverse propagation constant p such that $|pw| \ll 1$.

That two narrow plates can support a TM mode but not a TE mode for $|pw| \ll 1$ can be understood from the fact that the TM mode only gives rise to an axially directed current on the plates, whereas the TE mode gives rise to both an axially directed and a transversely directed current on the plates.

C. The Field Distribution of the TM Modes

So far, all efforts have been concentrated on the calculation of the transverse propagation constants. These calculations show how far each mode propagates from the point of excitation until it has been attenuated to an insignificant amplitude. In trying to understand the properties of the higher-order modes it is also important to have information on the transverse field associated with each mode.

In the following an investigation will be given of the transverse electric

and magnetic fields of the TEM mode and the three lowest order antisymmetric TM modes (those modes whose current distribution is of equal magnitude but opposite direction on the two plates). The TEM mode has been investigated extensively elsewhere[1,4] and so the field of this mode is included only for the sake of completeness.

The normalized electric field distribution $\underline{e}_0(x,y)$ of the TEM mode is given by

$$\underline{e}_0(x,y) = \frac{h}{2} \frac{x\hat{x}+(y+h)\hat{y}}{x^2+(y+h)^2} - \frac{h}{2} \frac{x\hat{x}+(y-h)\hat{y}}{x^2+(y-h)^2} \tag{39}$$

whereas the normalized magnetic field distribution is $\underline{h}_0(x,y) = \hat{z} \times \underline{e}_0(x,y)$. The normalized field distribution of the antisymmetric TM modes are given by

$$\underline{e}_n(x,y) = \frac{1}{2} \frac{x\hat{x}+(y+h)\hat{y}}{\sqrt{x^2+(y+h)^2}} \frac{K_1\left(p_n^- \sqrt{x^2+(y+h)^2}\right)}{K_1(p_n^- h)}$$

$$- \frac{1}{2} \frac{x\hat{x}+(y-h)\hat{y}}{\sqrt{x^2+(y-h)^2}} \frac{K_1\left(p_n^- \sqrt{x^2+(y-h)^2}\right)}{K_1(p_n^- h)} \tag{40}$$

$$\underline{h}_n(x,y) = \hat{z} \times \underline{e}_n(x,y)$$

and $\underline{e}_n(x,y)$ has been normalized such that $\underline{e}_n(0,0) = \hat{y}$.

The variation along the y-axis of the electric and magnetic fields of the TEM mode and the three lowest TM modes is shown in Fig. 4. This figure clearly shows that the field of each mode has an oscilliatory variation between the plates whereas outside the plates the field increases exponentially. The variation along the x-axis of the field is shown in Fig. 5. This figure shows that although the absolute value of the field is fairly constant the phase varies quite rapidly with the distance from the center of the simulator.

To get more understanding for the properties of the higher order modes, the transverse field lines of the TEM mode and the two lowest TM modes are shown in Figs. 6-8. It is noted from these figures that the magnetic field lines form

26

orthogonal trajectories to the transverse electric field lines. These mode patterns show a resemblance with those of the TM modes on a closed waveguide[11], the major difference being that the leaky modes are complex whereas the field components of an "ordinary" waveguide mode can be expressed in terms of a real function. The mode patterns in Figs. 6-8 mainly show the direction of the electric and magnetic fields of the modes. Therefore, as a complement to these plots the magnitude of the field of the TEM mode and the two lowest TM modes are portrayed in Figs. 9-11. Again it should be noticed that the absolute value of both the transverse and longitudinal fields increase almost monotonically away from the waveguide whereas the real and imaginary parts have both "peaks" and "valleys". Around the center of the waveguide the field of the lowest modes is reasonably uniform such that the normalized transverse electric field is in the y-direction, the normalized magnetic field is in the x-direction and that both fields are almost real. Finally, it should be pointed out that, of course, the transverse spatial variation is more rapid for modes with a large transverse propagation constant than for those with a small transverse propagation constant.
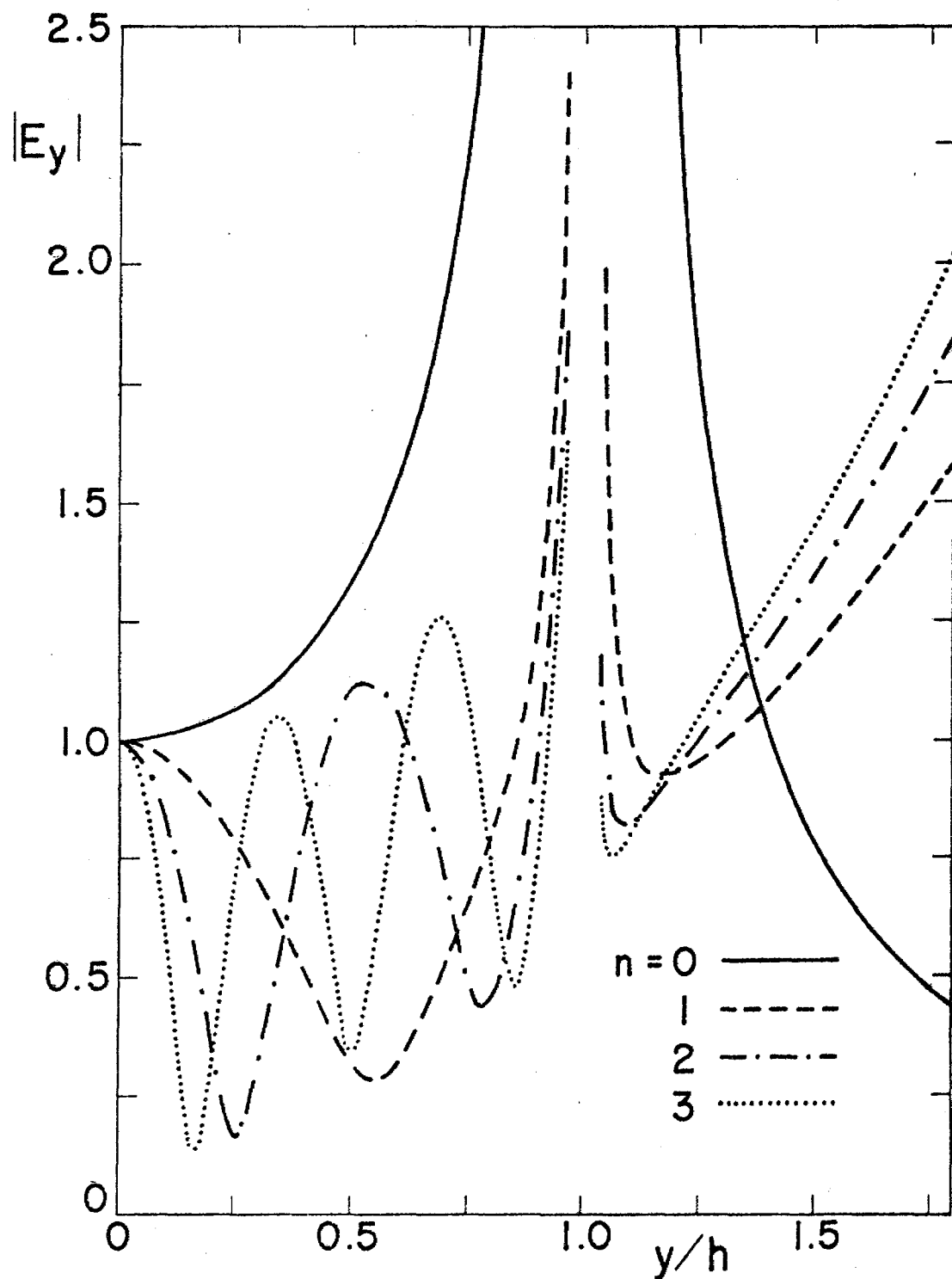
Figure 4a. The variation along the y-axis of the absolute value of the
normalized electric field for the TEM mode (n = 0) and the
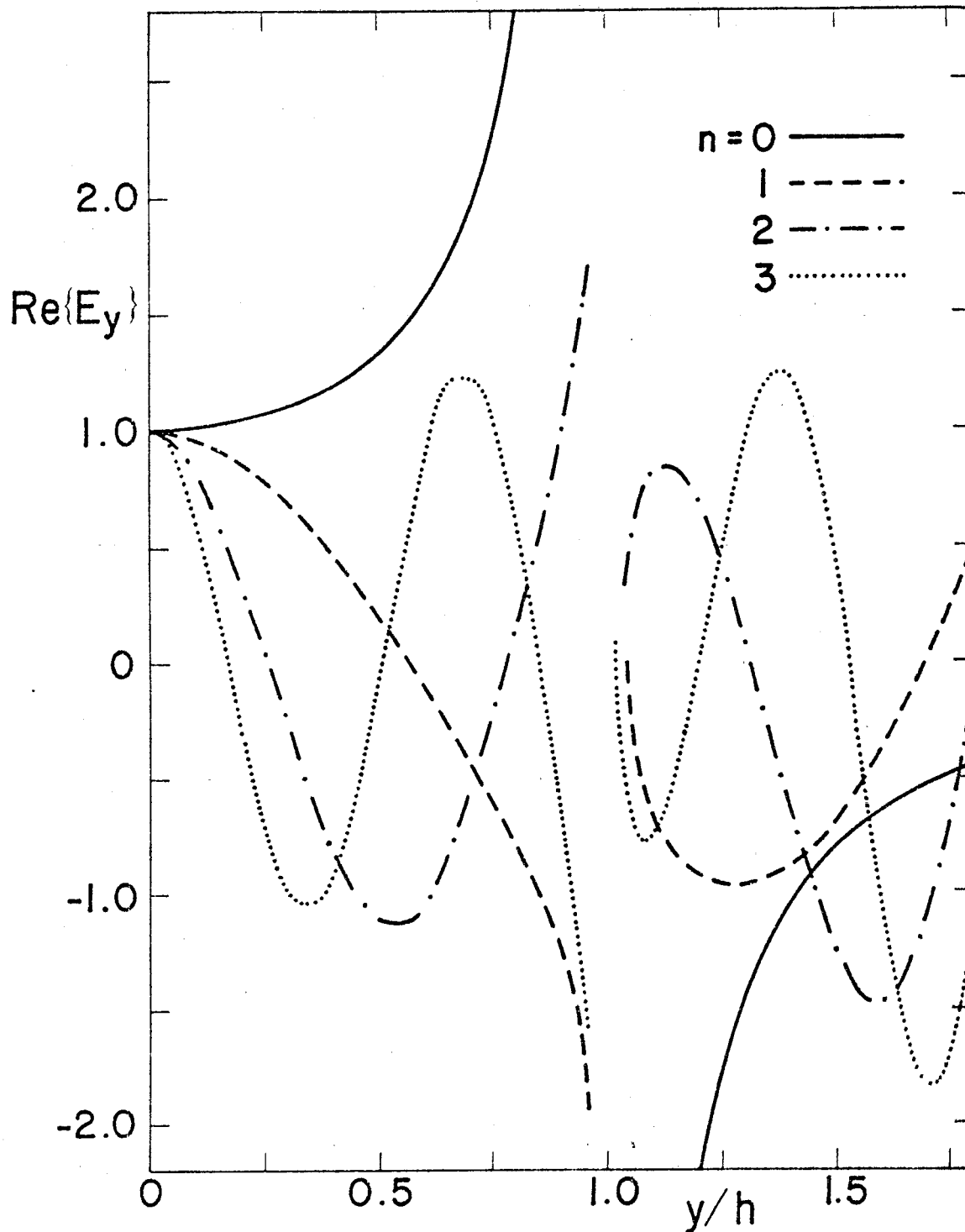lowest antisymmetric TM modes (n = 1,2,3). The plates are
located at y/h = ± 1.

Figure 4b. The variation along the y-axis of the real part of the normalized electric field for the TEM mode (n = 0) and the lowest anti-symmetric TM modes (n = 1,2,3). The plates are located at y/h = ± 1.
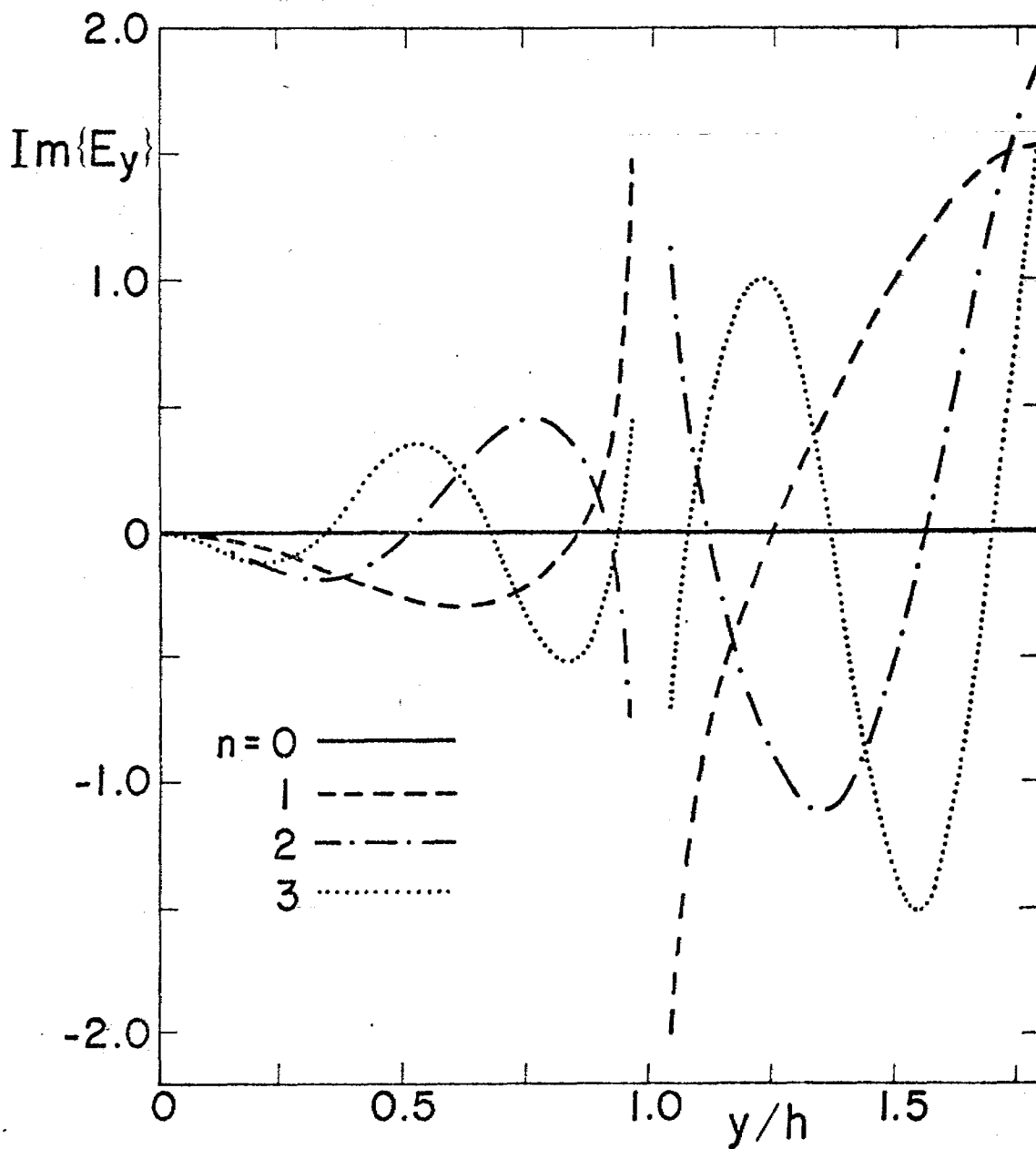
Figure 4c. The variation along the y-axis of the imaginary part of the
normalized electric field for the TEM mode   (n = 0)   and the
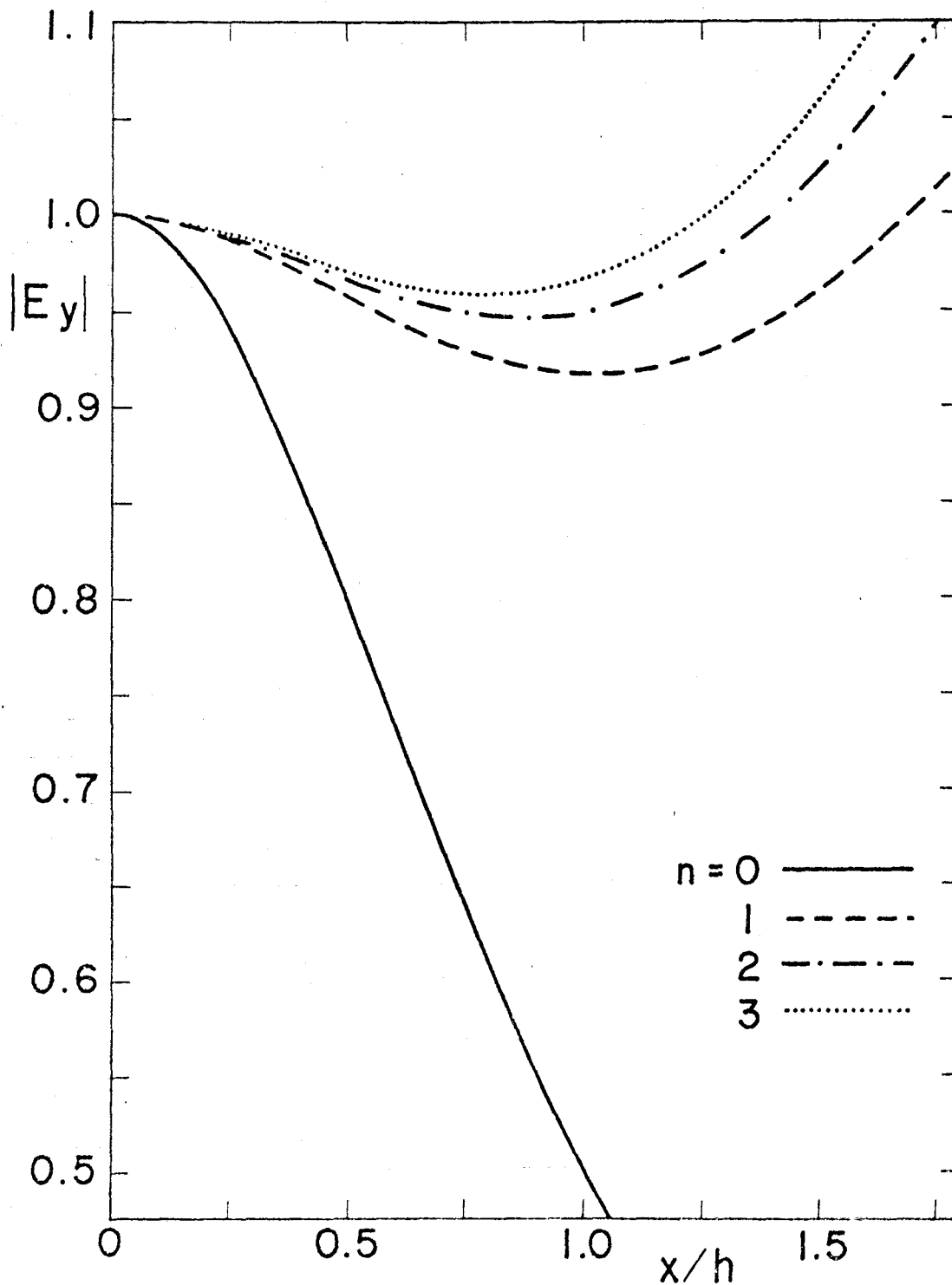lowest antisymmetric TM modes   (n = 1,2,3).   The plates are
located at   y/h = ± 1.

Figure 5a. The variation along the x-axis of the absolute value of the normalized electric field for the TEM mode (n = 0) and the lowest antisymmetric TM modes (n = 1,2,3). The plates are located at y/h = ± 1.

31

Figure 5b. The variation along the x-axis of the real part of the normalized electric field for the TEM mode (n = 0) and the lowest antisymmetric TM modes (n = 1,2,3). The plates are located at y/h = ± 1.

Figure 5c. The variation along the x-axis of the imaginary part of the normalized electric field for the TEM mode (n = 0) and the lowest antisymmetric TM modes (n = 1,2,3). The plates are located at y/h = ± 1.
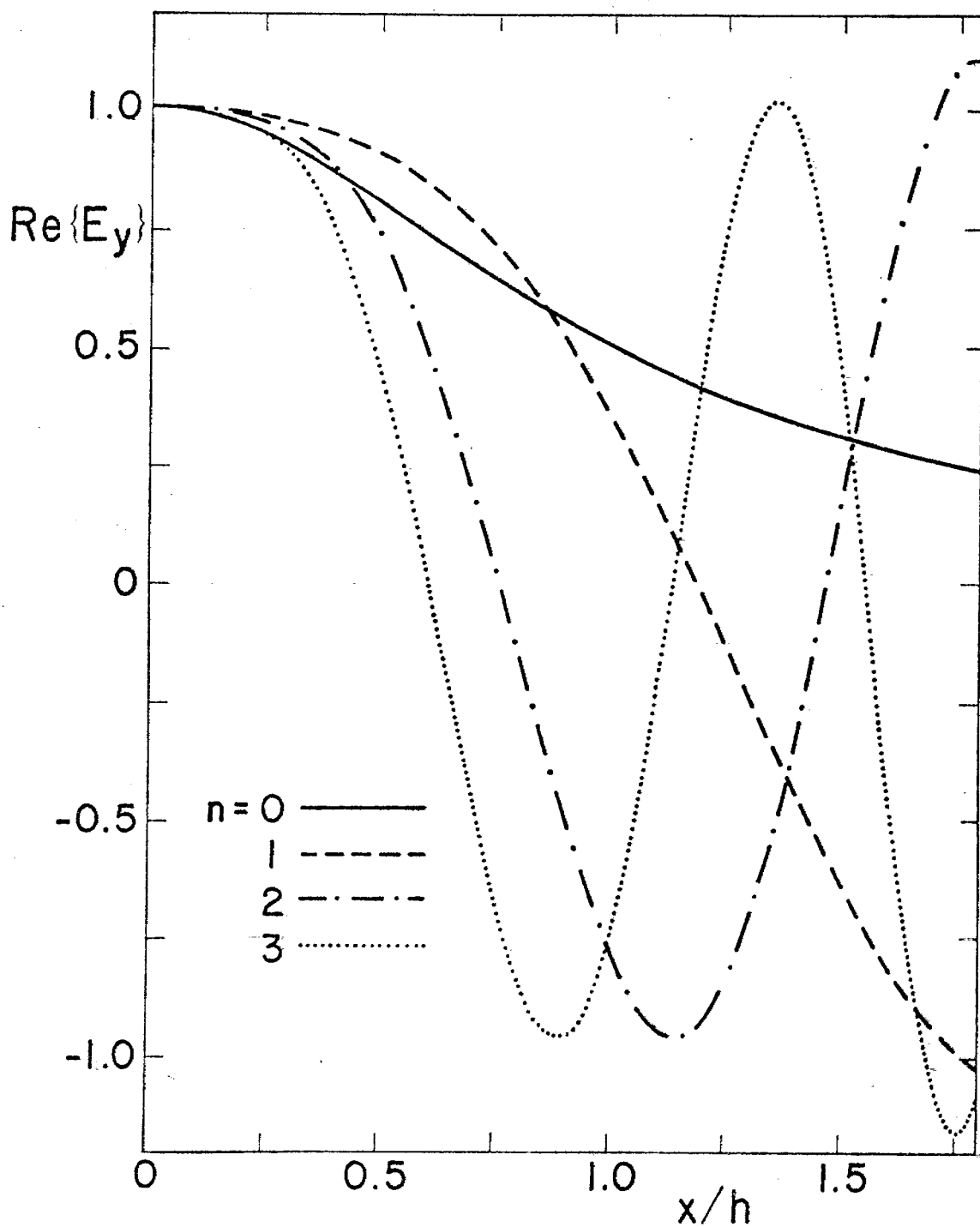
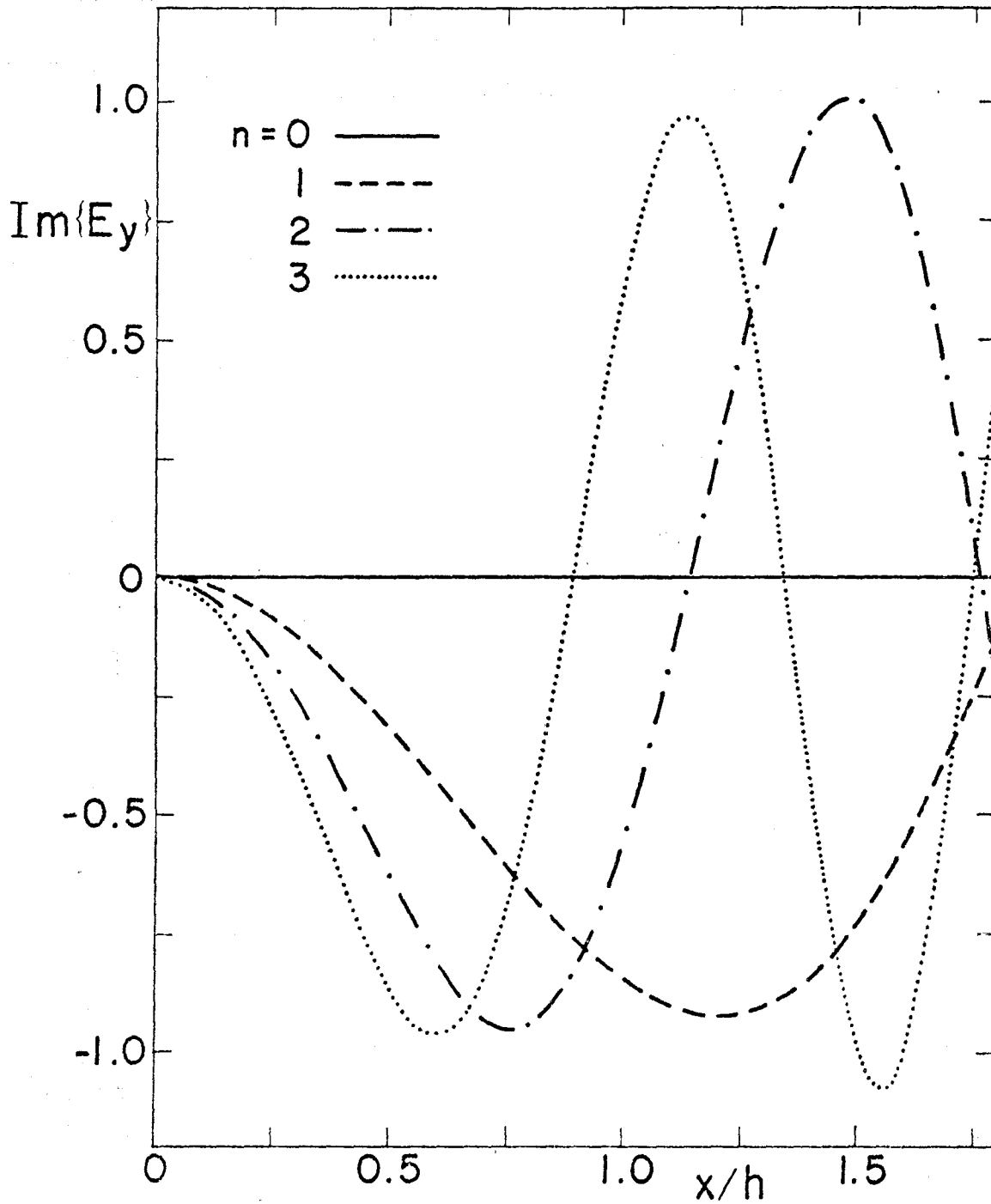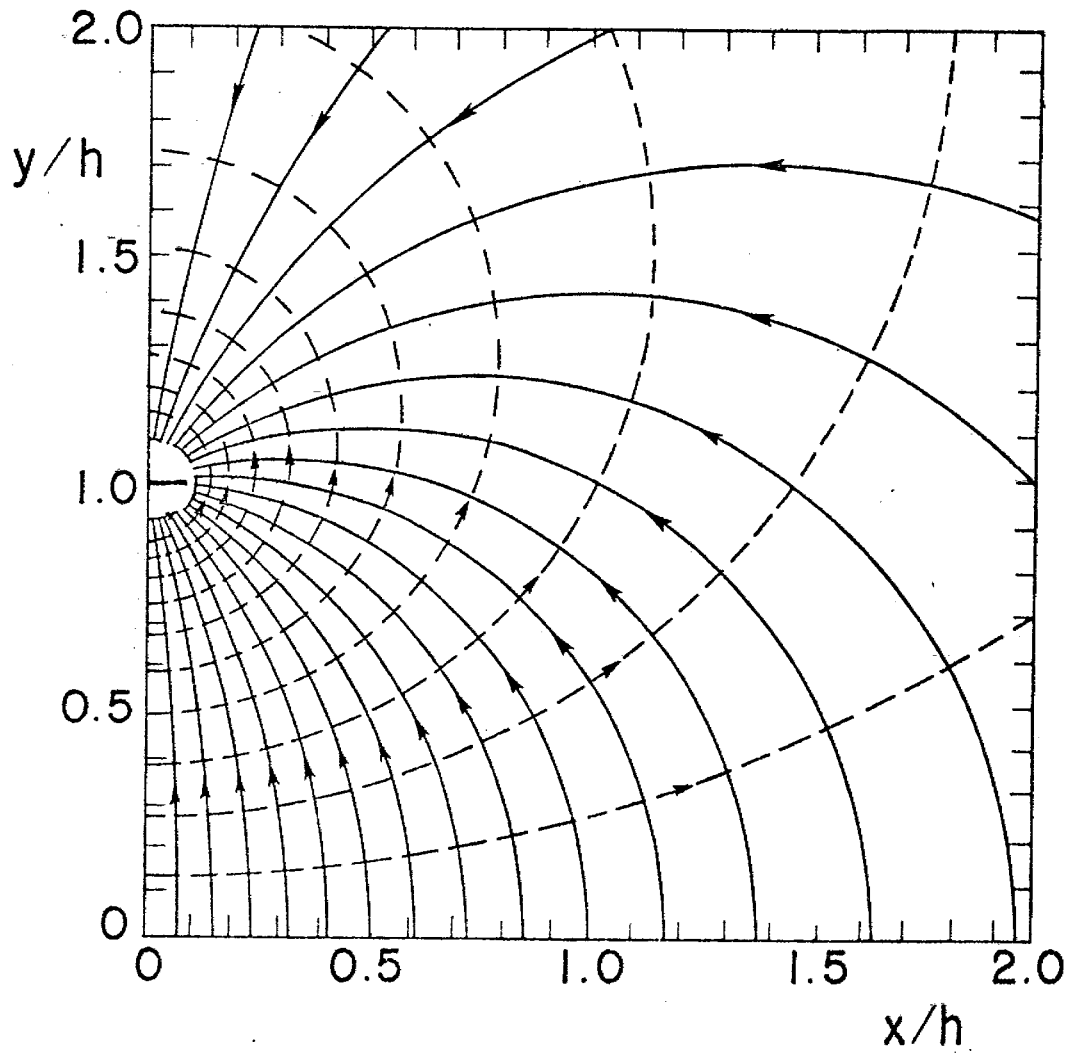Figure 6. The electric field lines (solid lines) and the magnetic field lines (broken lines) of the TEM mode.

Figure 7a. The electric field lines (solid lines) and the magnetic field
lines (broken lines) of the real part of the first antisymmetric
TM mode.
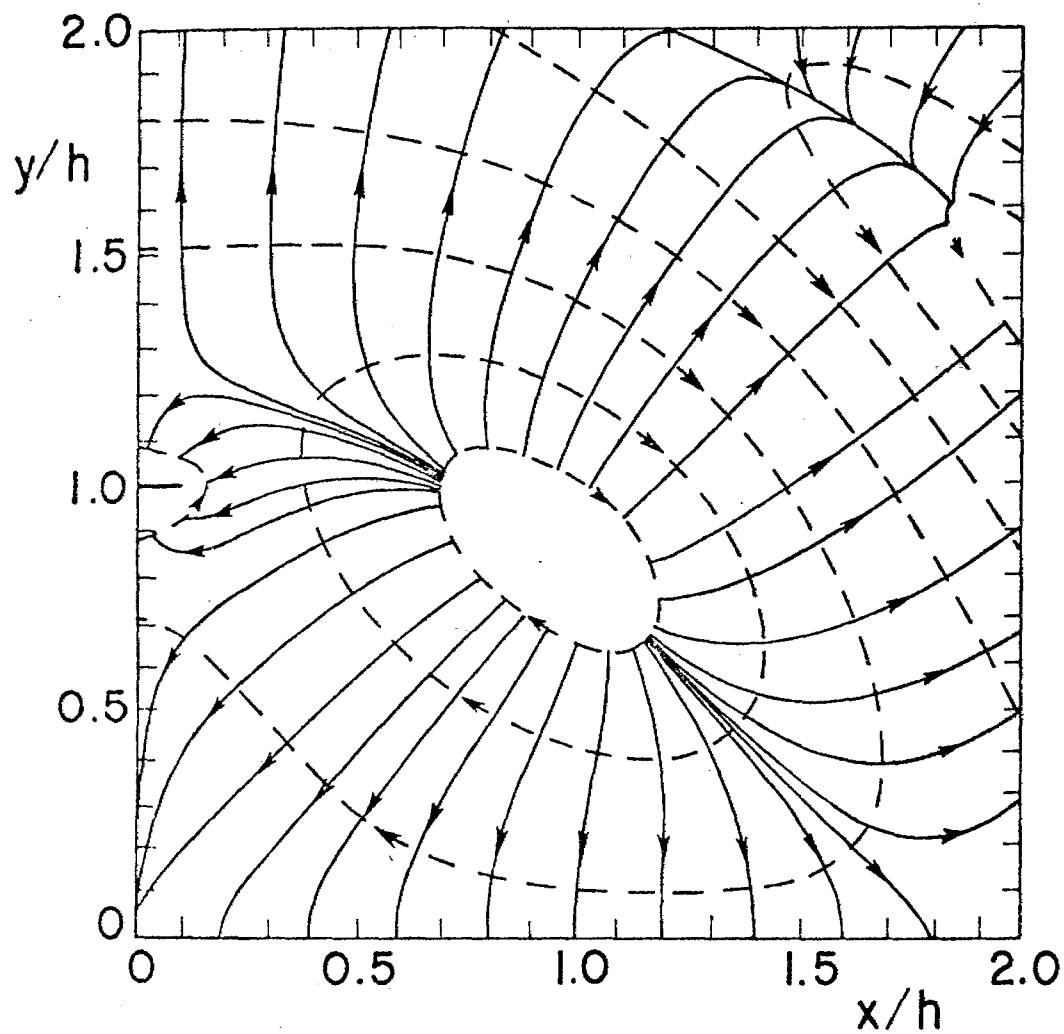
Figure 7b. The electric field lines (solid lines) and the magnetic field
lines (broken lines) of the imaginary part of the first anti-
symmetric TM mode.

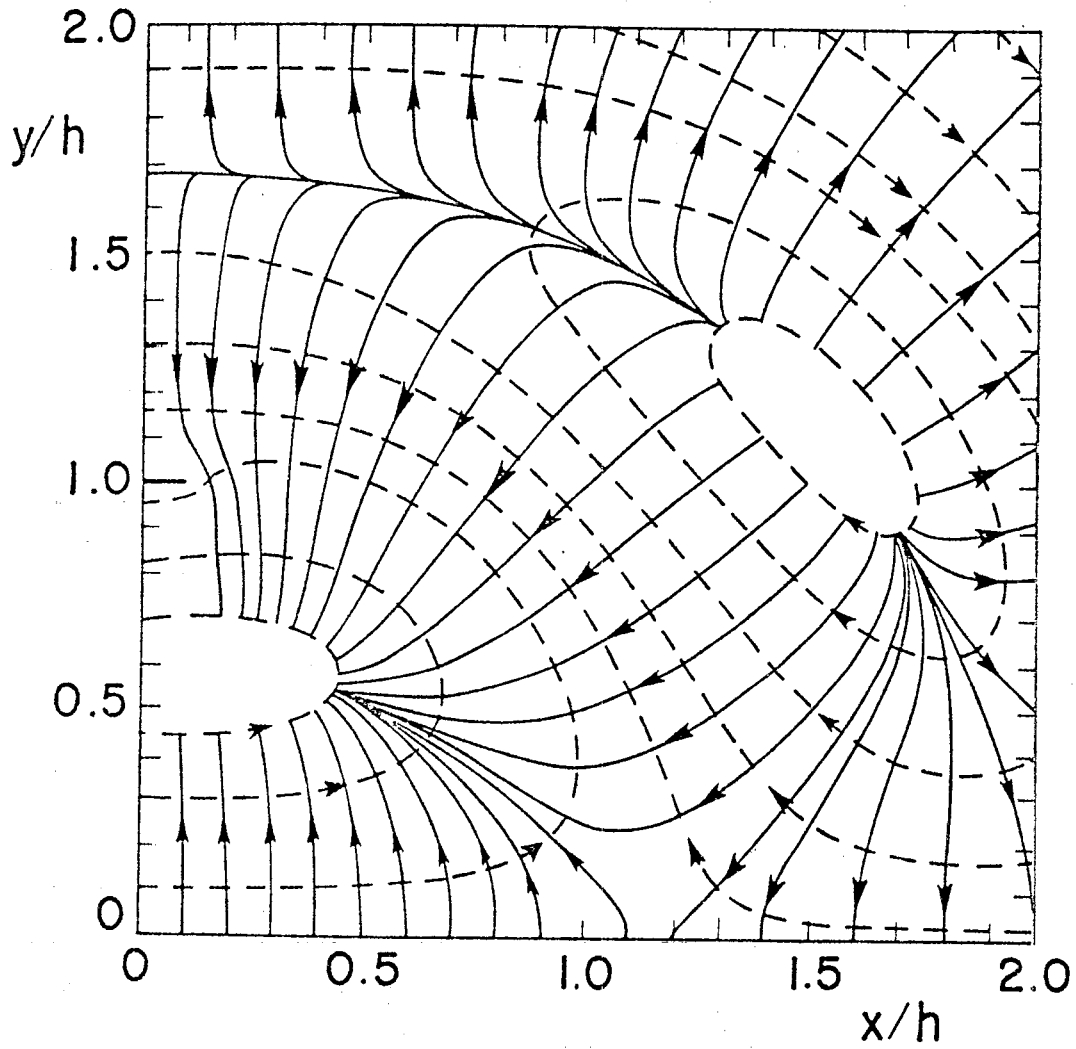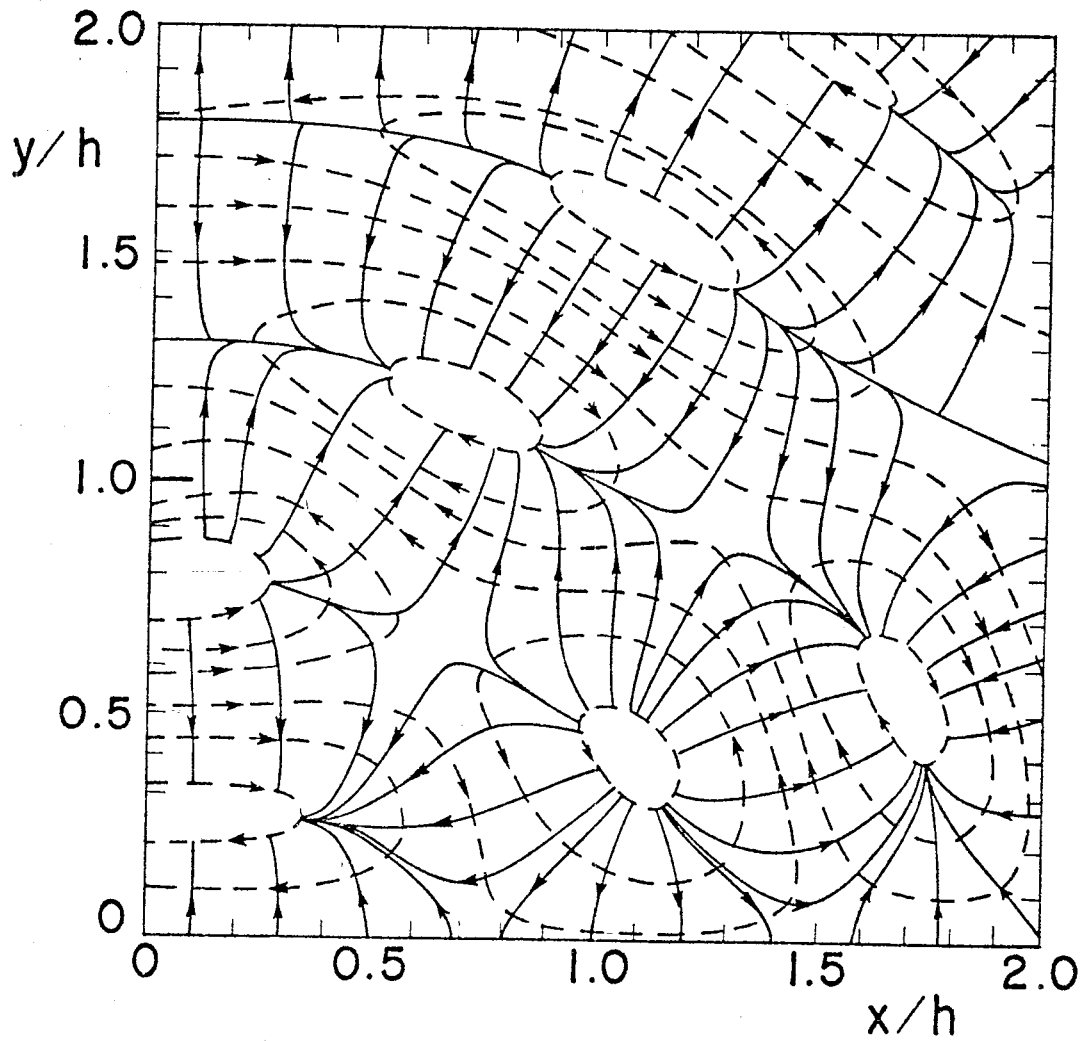Figure 8a. The electric field lines (solid lines) and the magnetic field lines (broken lines) of the real part of the second anti-symmetric TM mode.
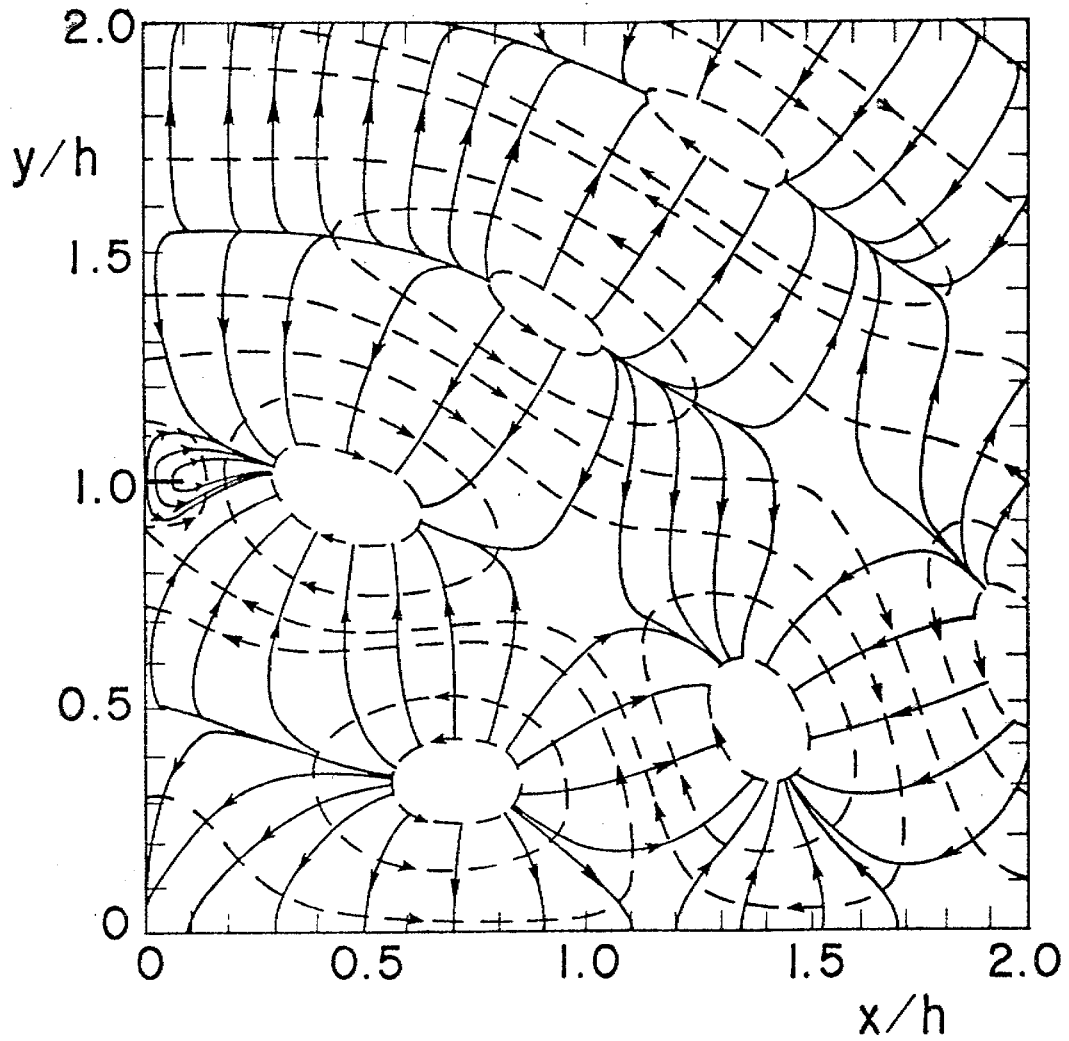
Figure 8b. The electric field lines (solid lines) and the magnetic field lines (broken lines) of the imaginary part of the second antisymmetric TM mode.
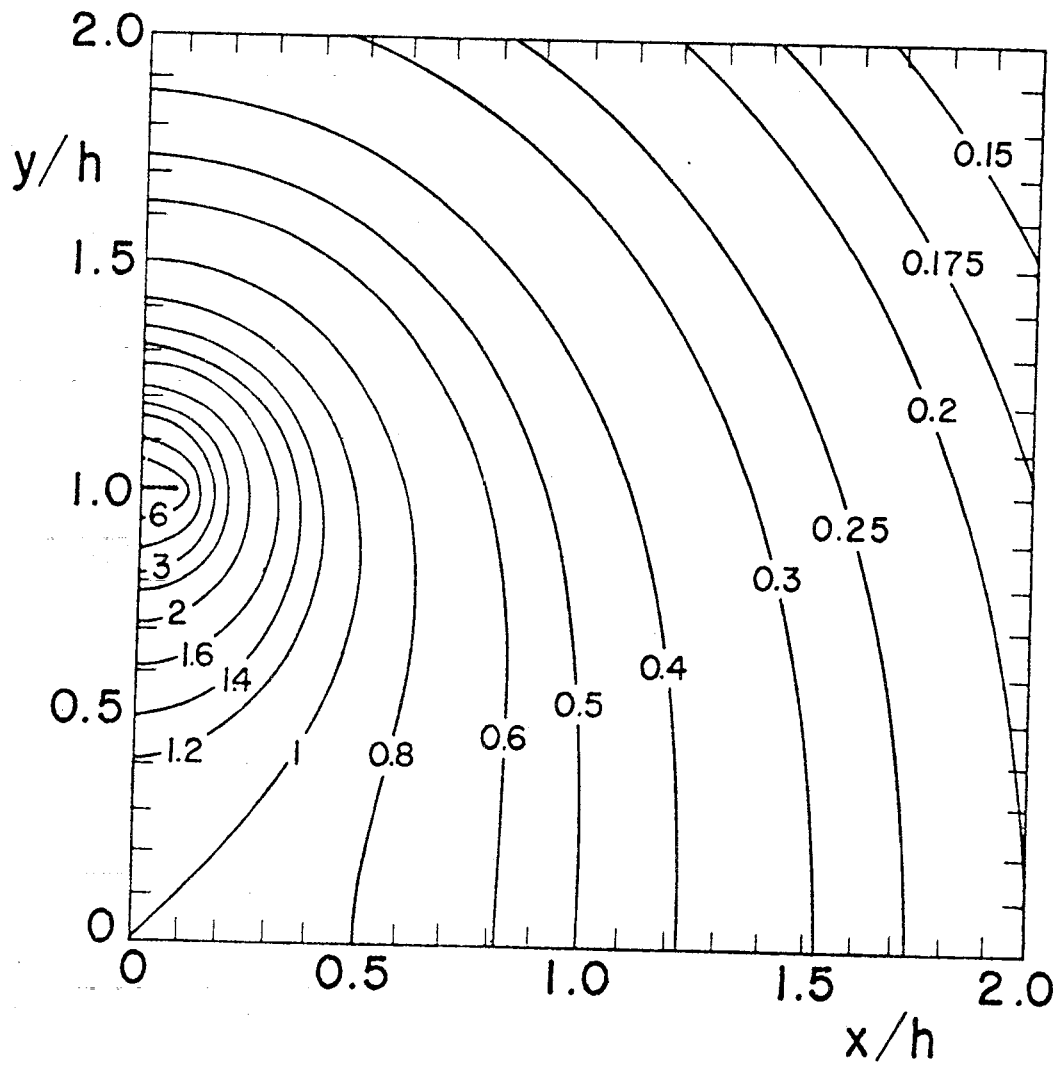
Figure 9. Lines of constant magnitude of the normalized electric and magnetic fields of the TEM mode.

Figure 10a. Lines of constant magnitude of the absolute value of the transverse part of the normalized electric and magnetic fields of the first TM mode.
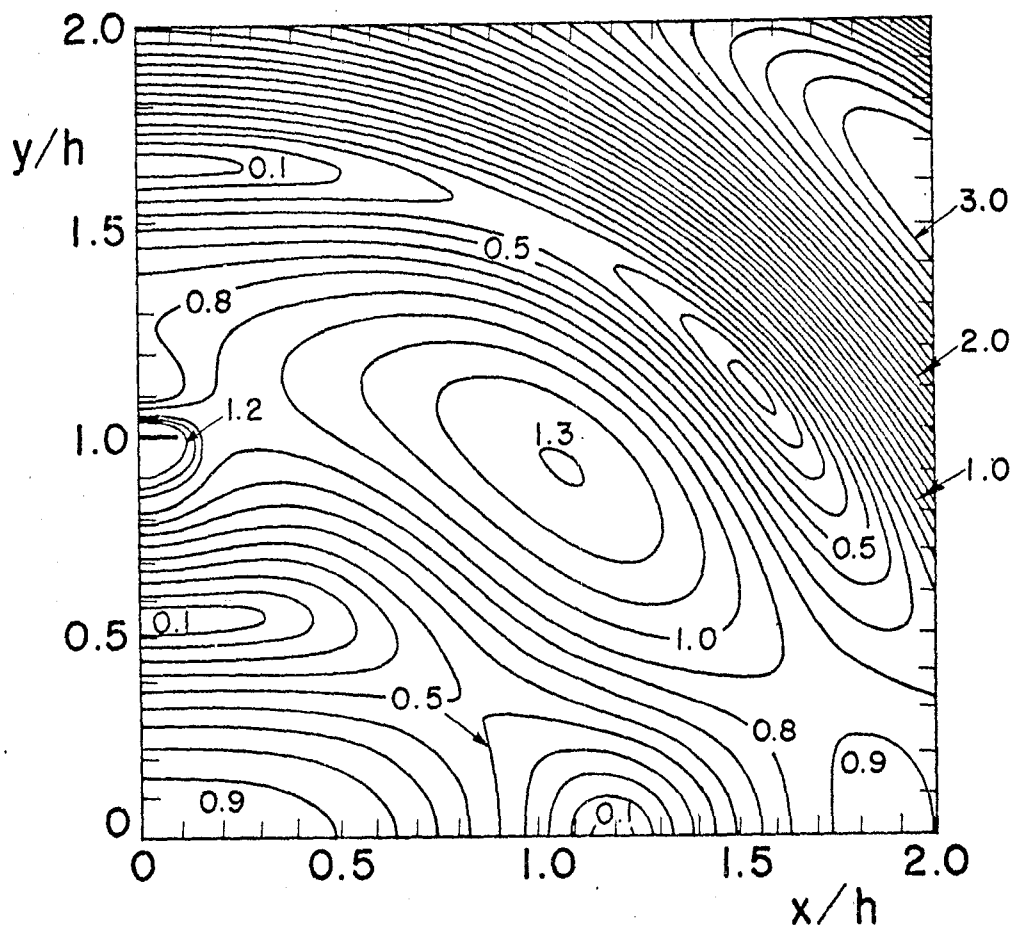
Figure 10b. Lines of constant magnitude of the real part of the transverse part of the normalized electric and magnetic fields of the first TM mode.
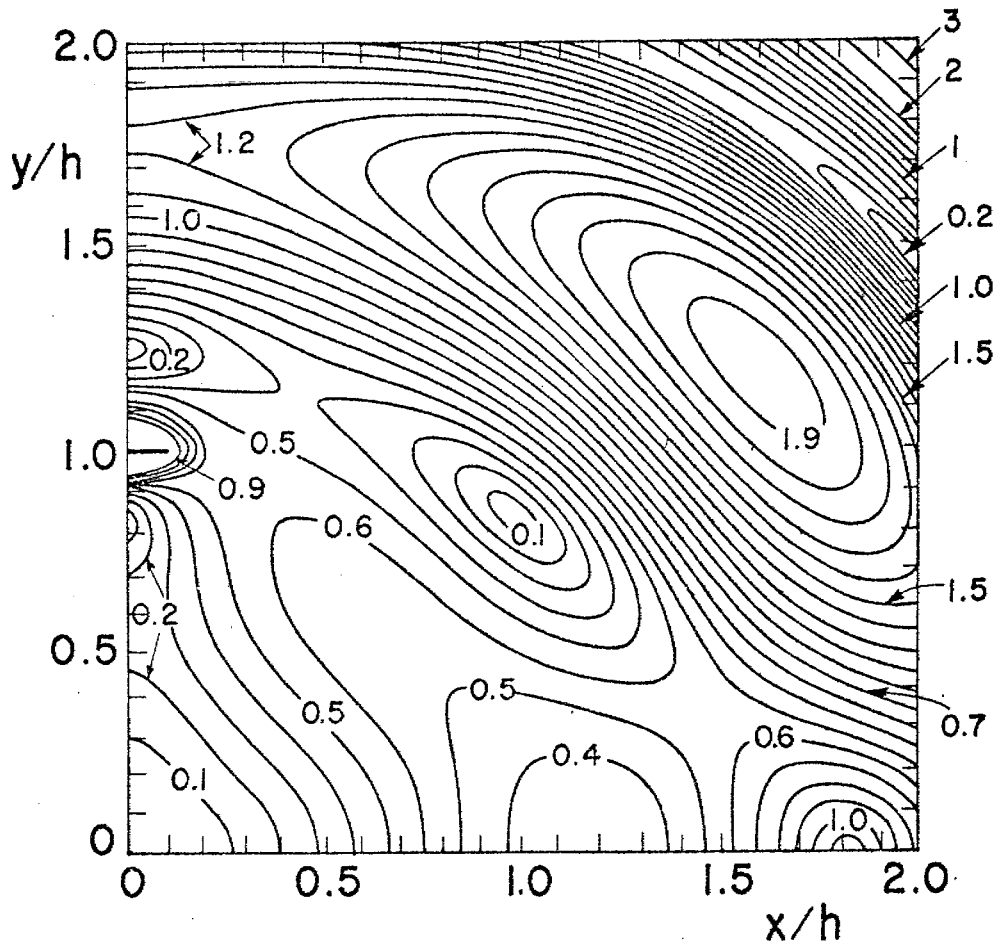
Figure 10c. Lines of constant magnitude of the imaginary part of the transverse part of the normalized electric and magnetic fields of the first TM mode.

Figure 10d. Lines of constant magnitude of the absolute value of the
longitudinal part of the normalized electric field of the
first TM mode.

Figure 10f. Lines of constant magnitude of the imaginary part of the longitudinal part of the normalized electric field of the first TM mode.
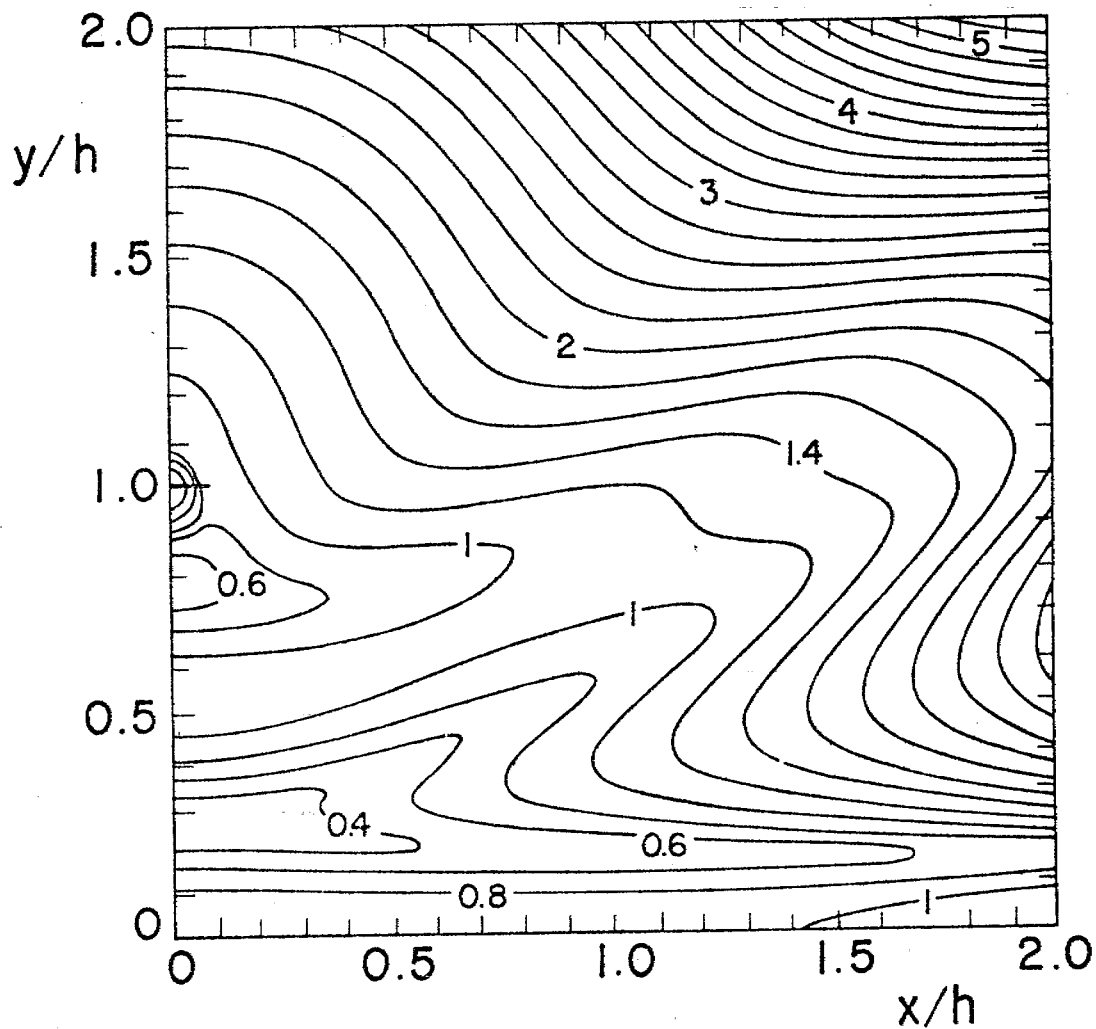
Figure 11a. Lines of constant magnitude of the absolute value of the transverse part of the normalized electric field of the second TM mode.

46
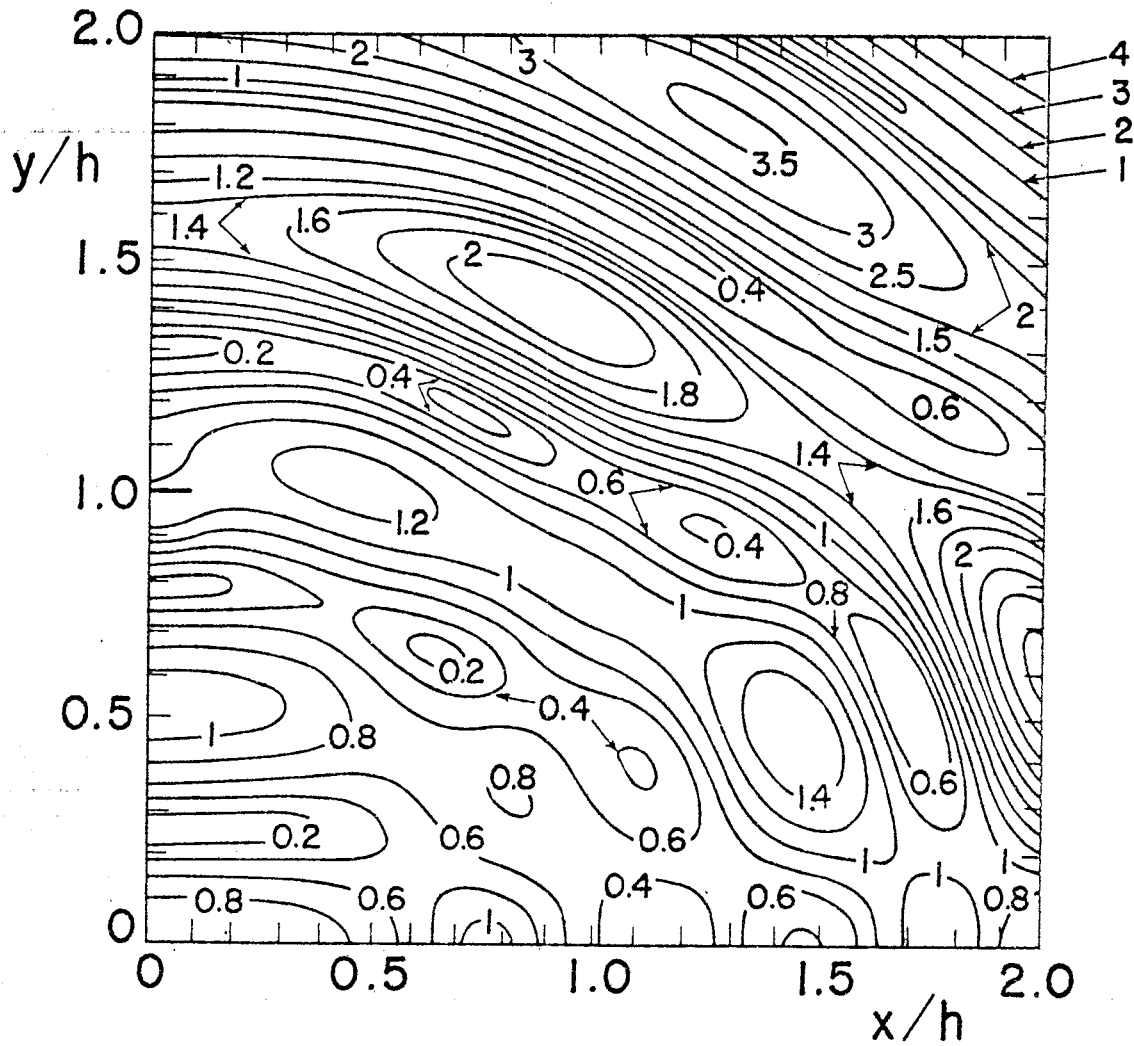
Figure 11b. Lines of constant magnitude of the real part of the transverse part of the normalized electric and magnetic fields of the second TM mode.

47
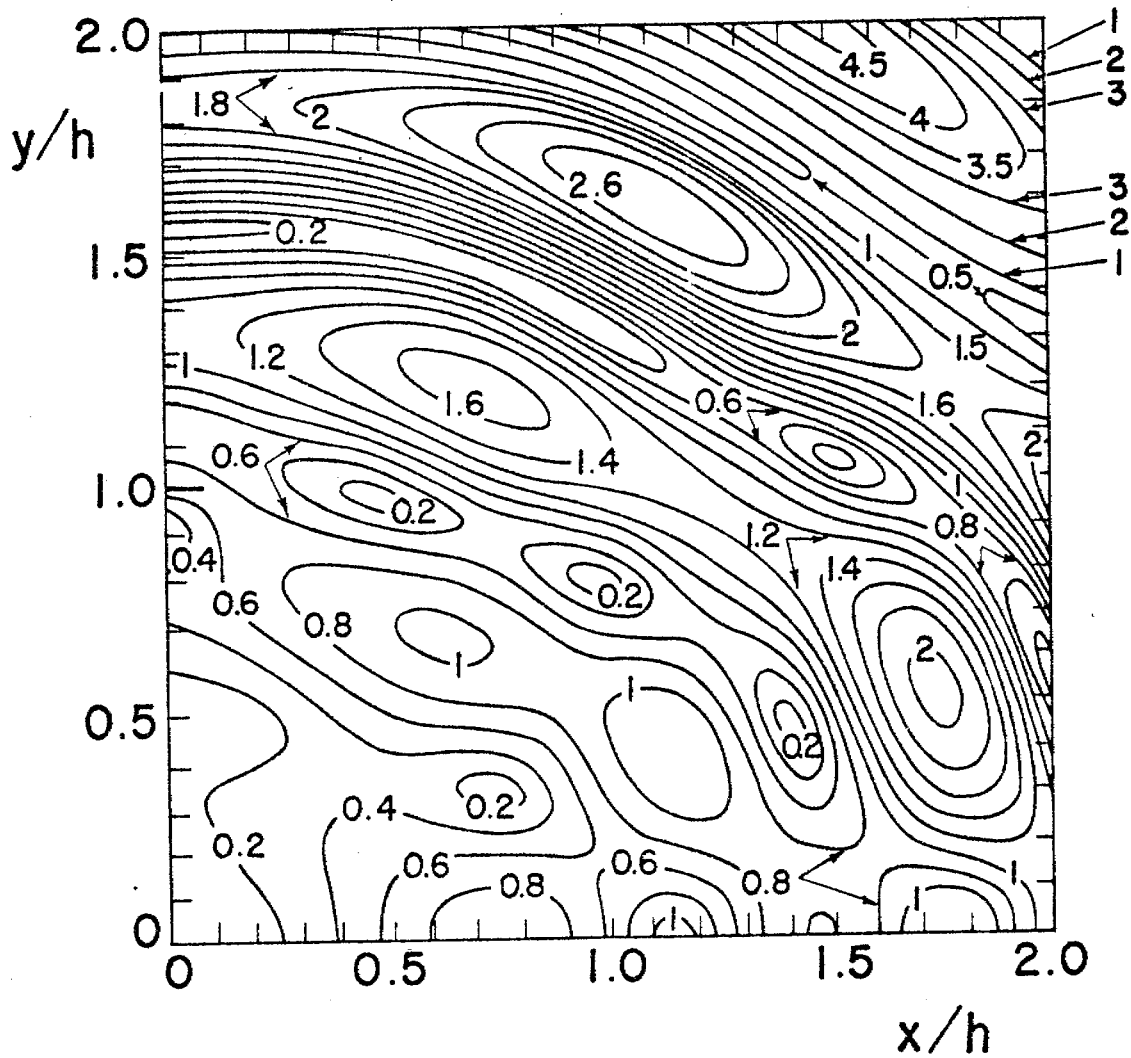
Figure 11c. Lines of constant magnitude of the imaginary part of the transverse part of the normalized electric and magnetic fields of the second TM mode.
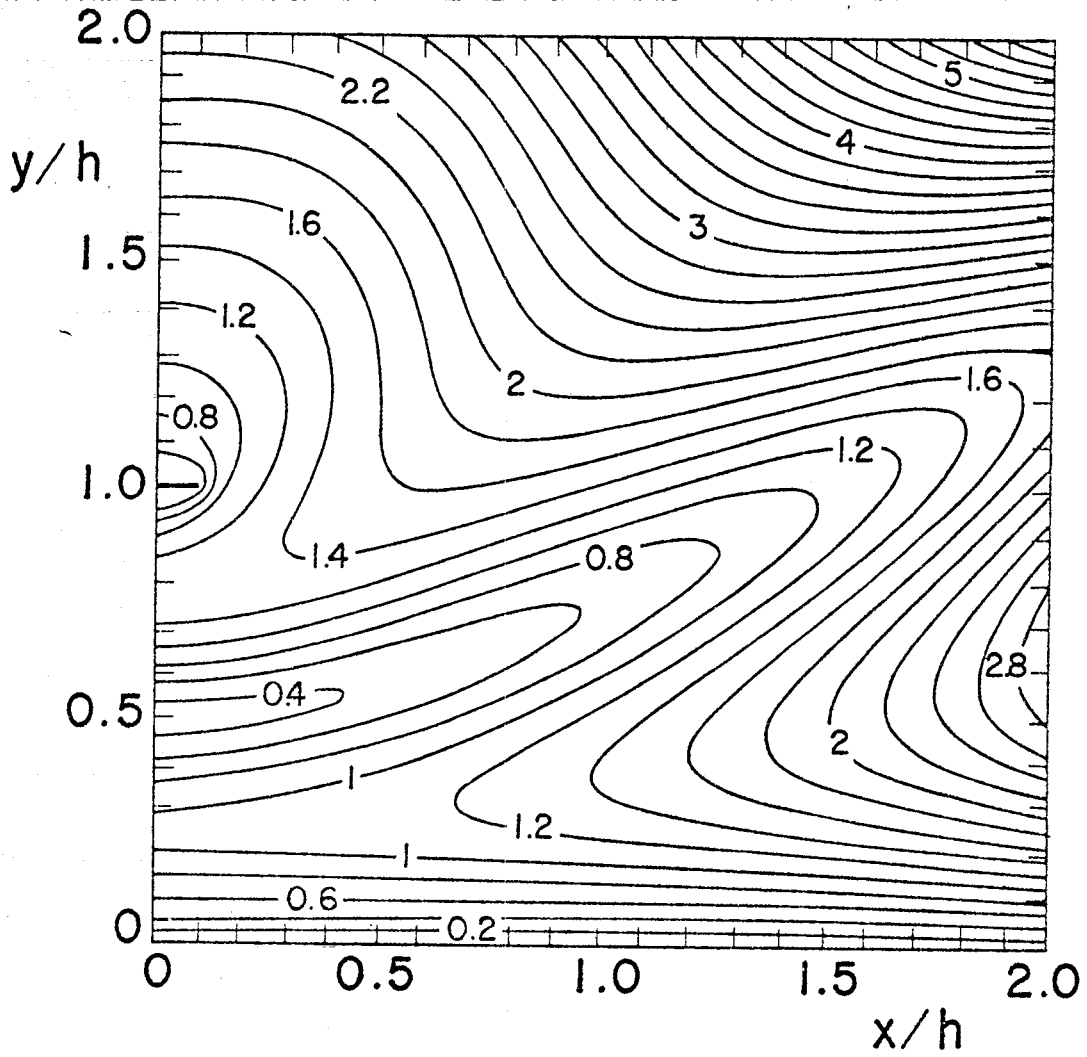
Figure 11d.   Lines of constant magnitude of the absolute value of the
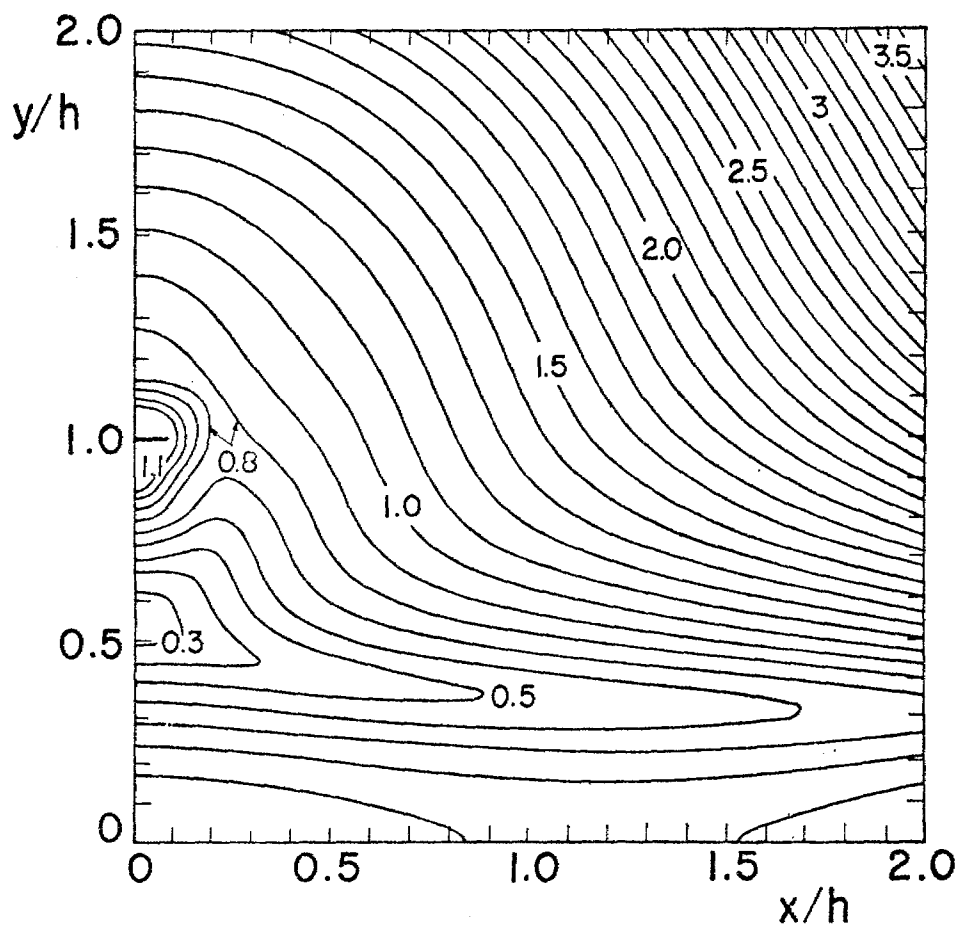longitudinal part of the normalized electric and magnetic fields
of the second TM mode.
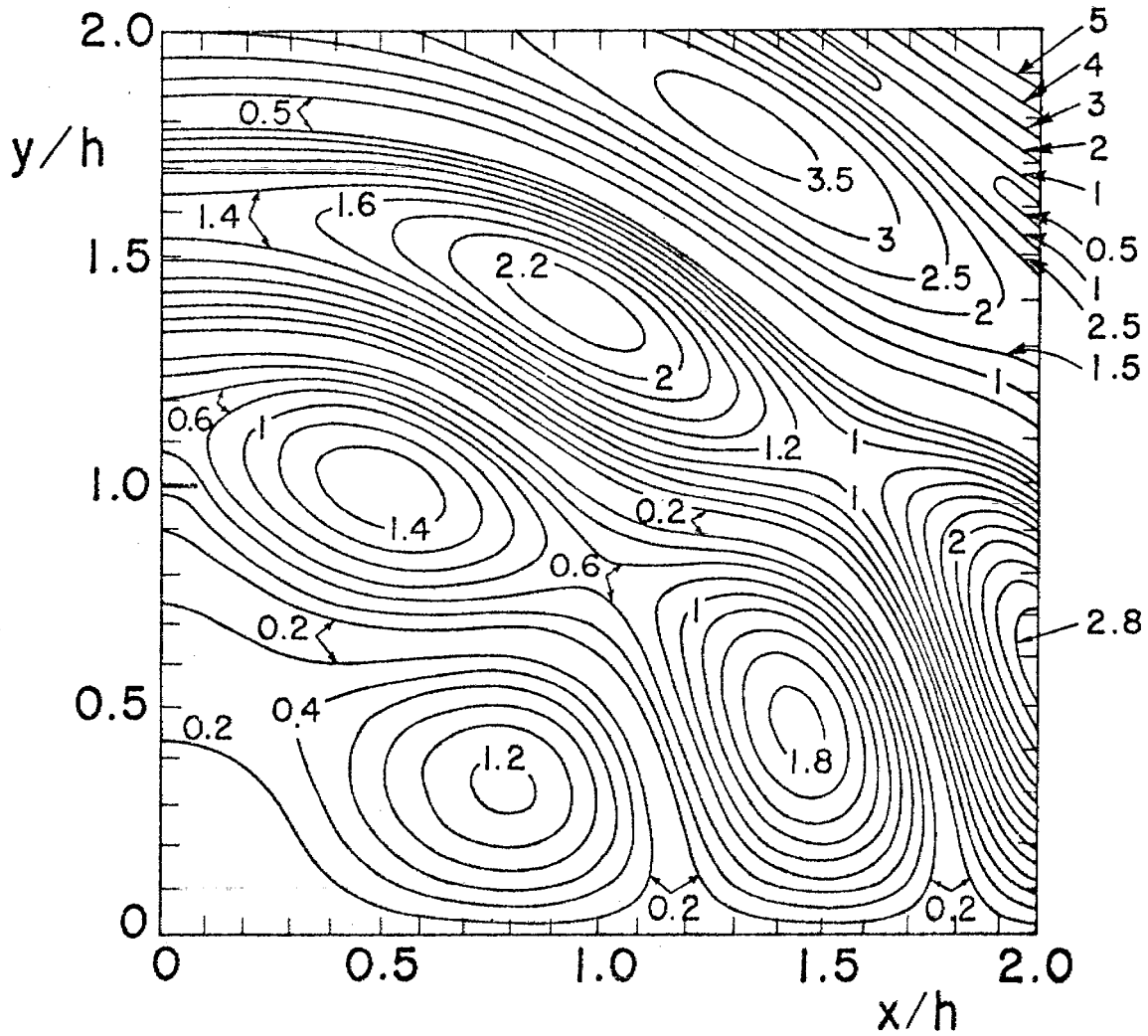
Figure 11e. Lines of constant magnitude of the real part of the longitudinal part of the normalized electric field of the second TM mode.
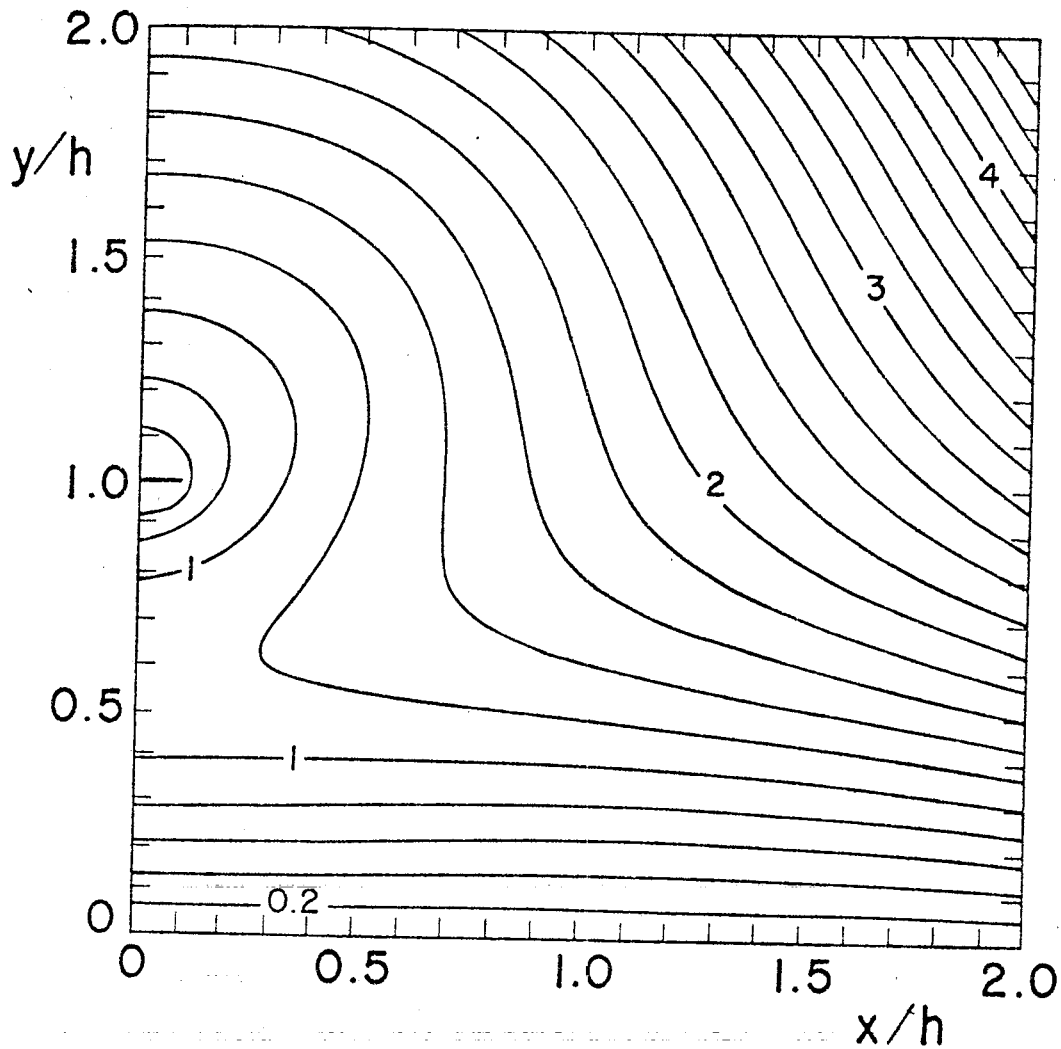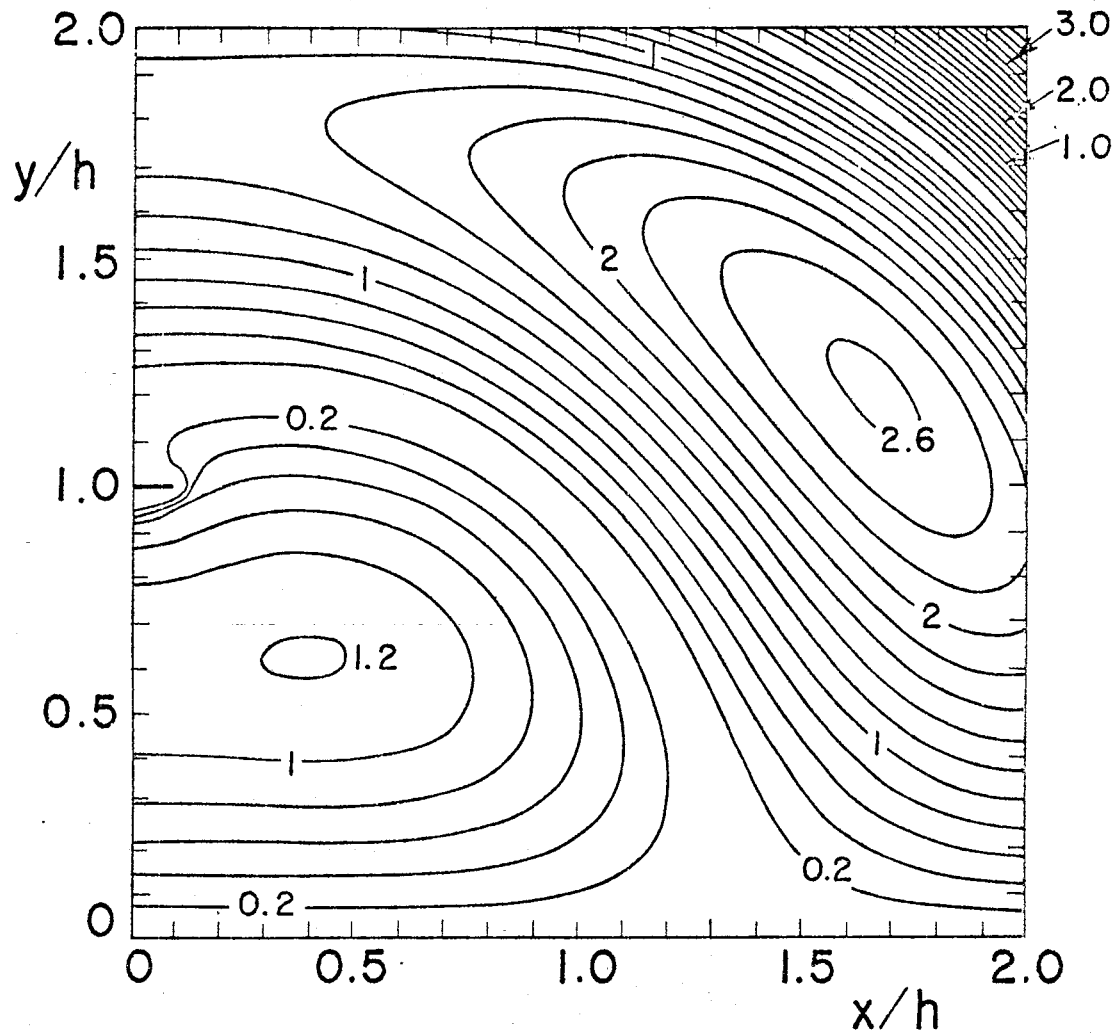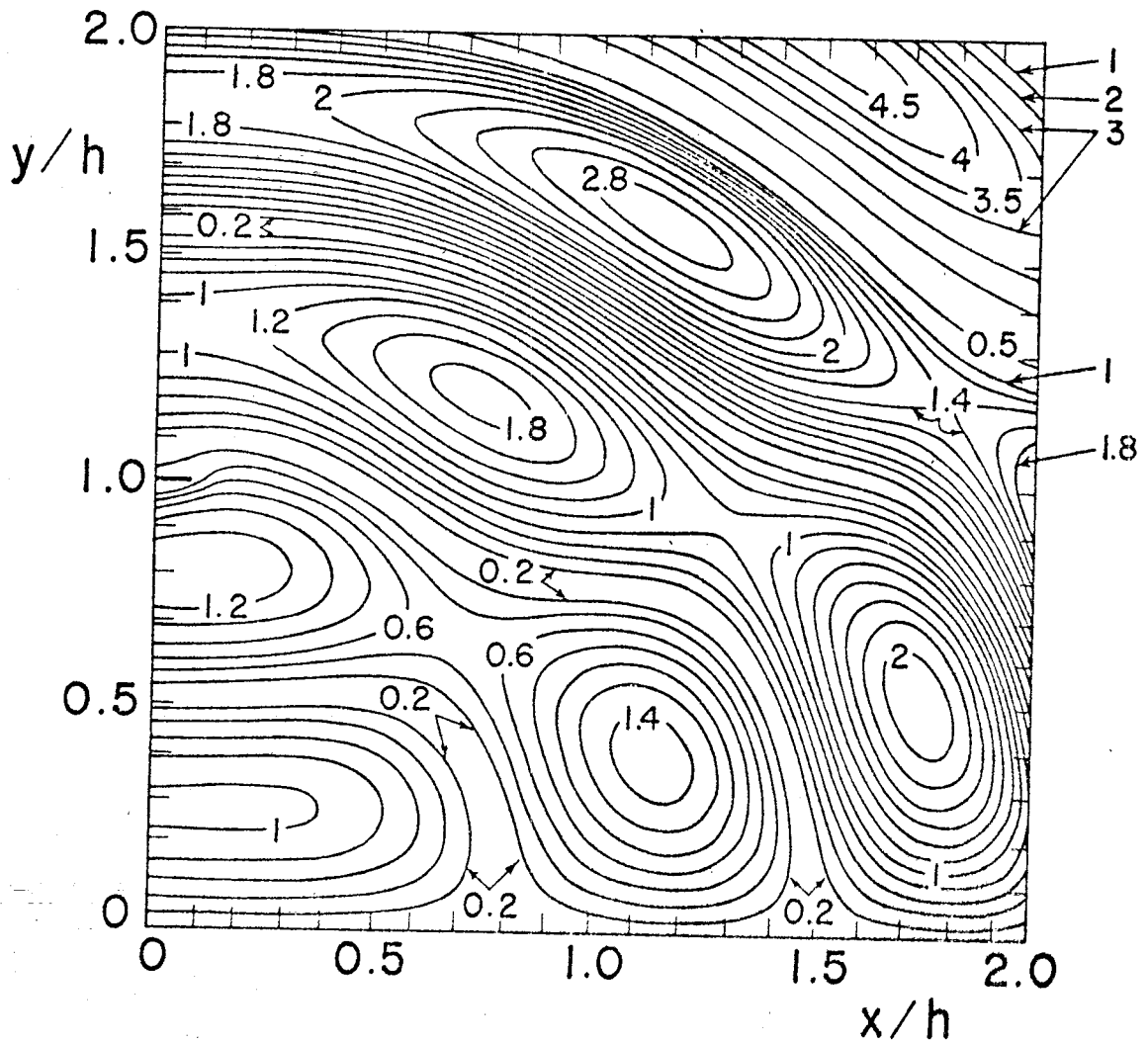
Figure 11f. Lines of constant magnitude of the imaginary part of the longitudinal part of the normalized electric field of the second TM mode.

V. Fredholm Integral Equation of the Second Kind
for the TM and TE Fields

In section II it was observed that the TM field (TE field) is obtained
by solving a two-dimensional scalar Dirichlet (Neumann) boundary-value problem.
These two boundary-value problems were then reduced to solving two integral
equations of the first kind. In the special case of narrow plates these integral
equations were solved analytically by first transforming them into Fredholm
integral equations of the second kind. In the general case of arbitrary
separation-to-width ratio of the plates the sets of integral equations (10) and
(12) cannot be solved using only analytical techniques. In this case one has to
resort to numerical methods and it is then important to start the numerical
calculations from an equation that is suitable for numerical treatment. To
this end an integral equation of the second kind will be derived in this section.

In Appendix A, scalar scattering from open surfaces is considered. Two
cases are treated, namely, (i) the case where the Dirichlet boundary condition
applies on the scattering surface and (ii) the case where the Neumann boundary
condition applies on the scattering surface. The results obtained in Appendix A
will be used in this section to derive integral equations of the second kind
for both the TM modes and the TE modes of two parallel plates of finite width.

A. Transverse Magnetic Modes

With the aid of the analysis in Appendix A, (c.f. (A9), (A14), and (A19))
one can derive the following homogeneous integral equations for the TM modes

$$u_{\pm}(x) - \int_{-W}^{W} L(x,x',0;p)u_{\pm}(x')dx' \mp \int_{-W}^{W} L(x,x',2h;p)u_{\pm}(x')dx' = 0 \qquad (41)$$

whereas the TE modes are determined by the nontrivial solutions of the "transposed"
integral equation

$$v_{\pm}(x) - \int_{-W}^{W} L(x',x,0;p)v_{\pm}(x')dx' \mp \int_{-W}^{W} L(x',x,2h;p)v_{\pm}(x')dx' = 0 \qquad (42)$$

where

$$L(x,x',y';p) = \frac{p}{\pi^2} \lim_{y \to 0} \frac{\partial}{\partial y} \left[\int_{-w}^{w} \frac{y}{\sqrt{(x-x'')^2+y^2}} K_1\left(p\sqrt{(x-x'')^2+y^2}\right) K_0\left(p\sqrt{(x'-x'')^2+y'^2}\right) dx'' \right.$$

$$\left. + \int_{-w}^{w} \frac{y+2h}{\sqrt{(x-x'')^2+(y+2h)^2}} K_1\left(p\sqrt{(x-x'')^2+(y+2h)^2}\right) K_0\left(p\sqrt{(x'-x'')^2+y'^2}\right) dx'' \right].$$

(43)

It was pointed out in Appendix A that the kernel in the integral equations
(41) and (42) has certain undesirable properties as far as the edge conditions
are concerned. It will later be shown explicitly how functions satisfying
certain edge conditions are transformed by the integral operators defined by
the kernels $L(x,x',y';p)$ and $L(x',x,y';p)$. But, first, consider an alternative
integral equation for $u_\pm(x)$, namely, the one that corresponds to (A32) in
Appendix A.

In the case of two parallel plates one can derive the following integral
equations from (A29) and (A32)

$$u_\pm(x) - \int_{-w}^{w} \hat{L}(x,x',0;p)u_\pm(x')dx' \mp \int_{-w}^{w} \hat{L}(x,x',2h;p)u_\pm(x')dx' = 0 \qquad (44)$$

where

$$\hat{L}(x,x',y';p) = p^2 \int_{-w}^{w} \text{sgn}(x''-x)K_1(p|x''-x|) \frac{x''-x'}{\sqrt{(x''-x')^2+y'^2}} K_1\left(p\sqrt{(x''-x')^2+y'^2}\right)dx''$$

$$+ p^2 \int_{-w}^{w} \left[\frac{x''-x}{\sqrt{(x''-x)^2+4h^2}} K_1\left(p\sqrt{(x''-x)^2+4h^2}\right) \right.$$

$$\times \left. \frac{x''-x'}{\sqrt{(x''-x')^2+(y'-2h)^2}} K_1\left(p\sqrt{(x''-x')^2+(y'-2h)^2}\right) \right] dx''$$

$$- p^2 \int_{-w}^{w} K_0(p|x''-x|)K_0\left(p\sqrt{(x''-x')^2+y'^2}\right) dx''$$

$$- p^2 \int_{-w}^{w} K_0\left(p\sqrt{(x''-x)^2+4h^2}\right)K_0\left(p\sqrt{(x''-x')^2+(y'-2h)^2}\right)dx'' . \qquad (45)$$

53

From this expression one notes that $\hat{L}(x,x',y';p)$ is a continuous function of x and x' when $y' \neq 0$ and that

$$\hat{L}(x,x',0;y) = \hat{L}_1(x,x';p) + \hat{L}_0(x,x';p)$$

$$\equiv \frac{1}{\pi^2} \int_{-w}^{w} \frac{dx''}{(x''-x)(x''-x')} + \hat{L}_0(x,x';p)$$

$$\equiv \frac{1}{\pi^2} \frac{1}{x-x'} \ln \frac{(w+x)(w-x')}{(w-x)(w+x')} + \hat{L}_0(x,x';p) \tag{46}$$

where $\hat{L}_0(x,x';p)$ is a continuous kernel. A relationship between the two kernels $L(x,x',y';p)$ and $\hat{L}(x,x',y';p)$ will be derived later.

Finally, it is of value to know how functions $u_\pm(x)$ that satisfy the appropriate edge conditons at $x = \pm w$ are transformed by an integral operator with the kernel $\hat{L}(x,x',0;p)$. Since the functions $u_\pm(x)$ are proportional to the charge density on each plate it is expected that the nontrivial solutions of (44) satisfy the edge conditions $u_\pm(x) \sim (w^2 - x^2)^{-\frac{1}{2}}$ as $x \to \pm w$. Indeed, the analysis in Appendix B shows that all nontrivial solutions of (44) must satisfy these edge conditions. One therefore concludes that (44) is suitable for numerical treatment.

Going back to the integral equation (41) one observes that the kernel in this integral equation can, with the aid of (A26), be cast into the form

$$L(x,x',y';p) = \hat{L}(x,x',y';p) - \pi^{-2}pK_1[p(w-x)]K_0\left(p\sqrt{(w-x')^2+y'^2}\right)$$

$$+ \pi^{-2}pK_1[p(w+x)]K_0\left(p\sqrt{(w+x')^2+y'^2}\right)$$

$$- \pi^{-2}p \frac{w-x}{\sqrt{(w-x)^2+4h^2}} K_1\left(p\sqrt{(w-x)^2+4h^2}\right)K_0\left(p\sqrt{(w-x')^2+(2h-y')^2}\right)$$

$$+ \pi^{-2}p \frac{w+x}{\sqrt{(w+x)^2+4h^2}} K_1\left(p\sqrt{(w+x)^2+4h^2}\right)K_0\left(p\sqrt{(w+x')^2+(2h-y')^2}\right) \tag{47}$$

54

from which it follows that

$$L(x,x',0;p) = \hat{L}_1(x,x';p) + \hat{L}_2(x,x';p) + \hat{L}_3(x,x';p)$$

$$\equiv \frac{1}{\pi^2} \frac{1}{x-x'} \ln\left[\frac{(w+x)(w-x')}{(w-x)(w+x')}\right] - \frac{1}{\pi^2} \frac{1}{w+x} \ln\left[\frac{w+x'}{w}\right]$$

$$+ \frac{1}{\pi^2} \frac{1}{w-x} \ln\left[\frac{w-x'}{w}\right] + \hat{L}_3(x,x';p) \tag{48}$$

where $\hat{L}_3(x,x';p)$ is a continuous function. From (48) it is noted that an integral operator with the kernel $\hat{L}_2(x,x';p)$ transforms any integrable function $u_\pm(x)$ into a function that behaves like $1/(w^2 - x^2)$ as $x \to \pm w$. Thus, the kernel $L(x,x',0;p)$ maps any function $u_\pm(x)$ that satisfies the edge conditions $u_\pm(x) \sim (w^2 - x^2)^{-\frac{1}{2}}$ as $x \to \pm w$ into a function with higher singularities at the edges. This feature of the kernel in (41) is considered undesirable and therefore the integral equation (44) is preferable to (41) when determining the properties of the TM modes on two parallel plates of finite width.

B.   Transverse Electric Modes

To find the properties of the TE modes one needs the solution of (42). For this reason the kernel $L(x',x,0;p)$ is first investigated,

$$L(x',x,0;p) = \frac{1}{\pi^2} \frac{1}{x-x'} \ln\left[\frac{(w+x)(w-x')}{(w-x)(w+x')}\right] - \frac{1}{\pi^2} \frac{1}{w+x'} \ln\left[\frac{w+x}{w}\right]$$

$$+ \frac{1}{\pi^2} \frac{1}{w-x'} \ln\left[\frac{w-x}{w}\right] + \hat{L}_3(x',x;p)$$

$$= \frac{1}{\pi^2} \frac{1}{w-x'} \frac{(w-x')\ln[(w-x')/w] - (w-x)\ln[(w-x)/w]}{x-x'}$$

$$- \frac{1}{\pi^2} \frac{1}{w+x'} \frac{(w+x')\ln[(w+x')/w] - (w+x)\ln[(w+x)/w]}{x-x'} + \hat{L}_3(x',x;p) \tag{49}$$

which shows that $L(x',\pm w,0;p)$ is an integrable function of x'. Putting $x = \pm w$ in (42) and noting that $v_\pm(\pm w) = 0$ one gets, after multiplication with $(w\pm x)/2$,

$$(w\pm x)/2 \left[\int_{-w}^{w} L(x',\pm w,0;p)v_{\pm}(x')dx' \pm \int_{-w}^{w} L(x',\pm w,2h;p)v_{\pm}(x')dx' \right] = 0. \qquad (50)$$

Combining (42) with (50) yields the following integral equation for $v_{\pm}(x)$,

$$v_{\pm}(x) - \int_{-w}^{w} \tilde{L}(x,x',0;p)v_{\pm}(x')dx' \mp \int_{-w}^{w} \tilde{L}(x,x',2h;p)v_{\pm}(x')dx' = 0 \qquad (51)$$

where

$$\tilde{L}(x,x',y;p) = L(x',x,y;p) - [(x+w)L(x',w,y;p) + (x-w)L(x',w,y;p)]/2.$$

By using methods similar to those employed in Appendix B one can show that the nontrivial solutions of (51) behaves like $v_{\pm}(x) \sim (w^2 - x^2)^{\frac{1}{2}}$ as $x \rightarrow \pm w$ which is in accordance with the edge conditions. It is therefore concluded that (51) is suitable for numerical calculations.

C. Numerical Solution of (44) and (51)

A brief discussion is now given of one method of solving (44) and (51). Starting with (44) one notes that the edge conditions and the properties of the kernel $\hat{L}(x,x',0;p)$ imply that it is feasible first to expand the unknown function $u_{\pm}(x)$ in the following series

$$u_{\pm}(x) = (w^2 - x^2)^{-\frac{1}{2}} \sum_{j=0}^{\infty} u_j^{\pm} T_j(x/w) \qquad (52)$$

where $T_j(\xi)$ is the first kind Chebysheff polynomial of degree j. To find the unknown coefficients $u_j^{\pm}$ one first substitutes the representation (52) for $u_{\pm}(x)$ into (44) and then multiplies this equation with $T_i(x/a)$ and integrates over the width of each plate (the method of moments). This procedure leads to the following set of simultaneous equations,

$$(\pi/2)\epsilon_i \delta_{ij} u_j^{\pm} - \sum_{j=0}^{\infty} [\hat{L}_{ij}(0;p) \pm \hat{L}_{ij}(2h;p)] u_j^{\pm} = 0, \qquad i = 0,1,2,\ldots \qquad (53)$$

56

where

$$\hat{L}_{ij}(y;p) = \int_{-w}^{w} \int_{-w}^{w} T_i(x/w)\hat{L}(x,x',y;p)(w^2 - x'^2)^{-\frac{1}{2}}T_j(x'/w)dx'dx$$

and δ_{ij} is the Kronecker symbol, $\delta_{ij} = 1$, $i = j$ and $\delta_{ij} = 0$, $i \neq j$ and $\varepsilon_i = 1 + \delta_{io}$.

Similarly, when using (51) to numerically determine the TE modes the edge conditions and the properties of $\tilde{L}(x,x',0;p)$ suggest that it is useful first to expand the unknown function $v_{\pm}(x)$ in the series

$$v_{\pm}(x) = (w^2 - x^2)^{\frac{1}{2}} \sum_{j=1}^{\infty} v_j^{\pm} U_j(x/w) \tag{54}$$

where $U_j(\xi)$ is the second kind Chebysheff polynomial of degree j. Again, by using moment methods one obtains the set of simultaneous algebraic equations for $v_j^{\pm}$,

$$(\pi/2)\delta_{ij}v_j^{\pm} - \sum_{j=0}^{\infty} [\tilde{L}_{ij}(0;p) \pm \tilde{L}_{ij}(2h;p)]v_j^{\pm} = 0, \qquad i = 1,2,3,\ldots \tag{55}$$

where

$$\tilde{L}_{ij}(y;p) = \int_{-w}^{w} u_i(x/w)\tilde{L}_{ij}(x,x',2h;p)(w^2 - x'^2)^{\frac{1}{2}}u_j(x'/w)dxdx'.$$

To numerically determine the transverse propagation constants and the field distributions of the TM and TE modes the sets of equations (53) and (55) are truncated to form a set of N equations for N unknowns. These numerical aspects of the problem will be left to future work where the methods outlined above are intended to be used when determining the properties of the TM and TE modes.

Fredholm Integral Equation of the Second Kind for
Scattering From Open Surfaces

It is well known that scattering from an open, infinitely thin surface can be reduced to integral equations or integral-differential equations of the first kind. From both theoretical and computational standpoints it is of great value to reduce the scattering problem to a Fredholm integral equation of the second kind. In this appendix scalar scattering from open surfaces will be considered. The Dirichlet as well as the Neumann boundary conditions are considered and the results are valid in both three and two dimensions.

A. Dirichlet Boundary Conditions

Let an open surface S with boundary L be illuminated by an incident scalar field $\phi_0(\underline{r})$. The scattered field $\phi(\underline{r})$ these satisfies the Helmholtz equation outside $S + L$,

$$\nabla^2 \phi - p^2 \phi = 0 \tag{A1}$$

and the boundary conditions

$$\phi^+(\underline{r}) = \phi^-(\underline{r}) = -\phi_0(\underline{r}), \qquad \underline{r} \in S \tag{A2}$$

where $\phi^+(\underline{r})$ $(\phi^-(\underline{r}))$ denotes the limiting value of $\phi(\underline{r})$ as $\underline{r}$ approaches a point on S from the positive (negative) side of S (see Fig.12). By applying the Green's theorem on the region outside $S + L$ and noting that ϕ satisfies the Sommerfeld radiation condition at infinity one gets

$$\phi(\underline{r}) = -\int_S G(\underline{r},\underline{r}')f(\underline{r}')dS' \tag{A3}$$

where

$$f(\underline{r}) = \frac{\partial \phi^+}{\partial n}(\underline{r}) - \frac{\partial \phi^-}{\partial n}(\underline{r}) , \qquad \underline{r} \in S \tag{A4}$$

58

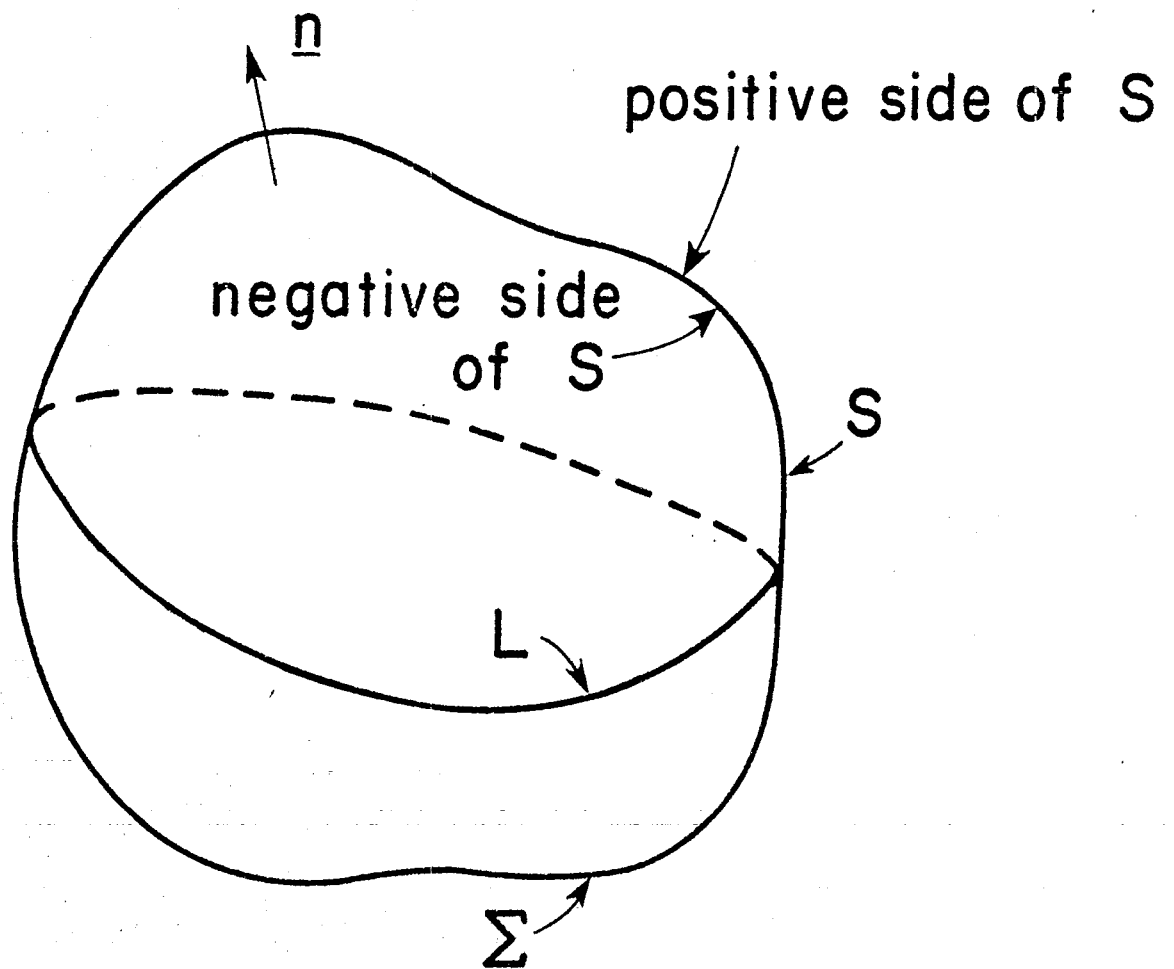Figure 12. The surfaces S, Σ, S_o and the boundary curve L.

$G(\underline{r},\underline{r}')$ is the free space Green's function,

$$G(\underline{r},\underline{r}') = \frac{\exp(-p|\underline{r}-\underline{r}'|)}{4\pi|\underline{r}-\underline{r}'|} \qquad \text{in 3 dimensions}$$

(A5)

$$G(\underline{r},\underline{r}') = \frac{K_0(p|\underline{r}-\underline{r}'|)}{2\pi} \qquad \text{in 2 dimensions}$$

and $K_0(x)$ is the modified Bessel function.

First, complete the surface S with an other open surface Σ having the boundary L so that $S + \Sigma$ forms a closed surface S_0. Next, by applying the Green's theorem to the region outside S_0 one gets

$$\frac{1}{2}\frac{\partial\phi^+}{\partial n}(\underline{r}) = \frac{\partial}{\partial n}\int_{S_0}\frac{\partial G}{\partial n'}(\underline{r},\underline{r}')\phi^+(\underline{r}')dS' - \int_{S_0}\frac{\partial G}{\partial n}(\underline{r},\underline{r}')\frac{\partial\phi^+}{\partial n'}(\underline{r}')dS',$$

$$\underline{r}\in S_0, \qquad (A6)$$

which combined with (A3) and (A4) results in

$$\frac{1}{2}\frac{\partial\phi^+}{\partial n}(\underline{r}) = -\frac{\partial}{\partial n}\int_{S}\frac{\partial G}{\partial n'}(\underline{r},\underline{r}')\phi_0(\underline{r}')dS' - \int_{\Sigma}\frac{\partial^2 G}{\partial n\partial n''}(\underline{r},\underline{r}'')dS''\int_{S}G(\underline{r}'',\underline{r}')f(\underline{r}')dS'$$

$$+ \int_{S_0}\frac{\partial G}{\partial n}(\underline{r},\underline{r}'')dS''\int_{S}\frac{\partial G}{\partial n''}(\underline{r}'',\underline{r}')f(\underline{r}')dS', \qquad \underline{r}\in S_0. \qquad (A7)$$

Similarly, by applying the Green's theorem to the region inside S_0 one derives an expression for $\partial\phi^-/\partial n$ which is given by (A7) provided that the following substitution is made in the left-hand side of (A7),

$$\frac{\partial\phi^+}{\partial n} \rightarrow -\frac{\partial\phi^-}{\partial n}. \qquad (A8)$$

By adding the two integral expressions thus obtained for $\partial\phi^\pm/\partial n$ one arrives at the following integral equation of the second kind for $f(\underline{r})$,

$$\frac{1}{4}f(\underline{r}) - \int_{S}L(\underline{r},\underline{r}')f(\underline{r}')dS' = f_0(\underline{r}), \qquad \underline{r}\in S \qquad (A9)$$

60

where

$$f_o(\underline{r}) = -\frac{\partial}{\partial n} \int_S \frac{\partial G}{\partial n'} (\underline{r},\underline{r}')\phi_o(\underline{r}')dS, \qquad \underline{r} \in S \tag{A10}$$

and

$$L(\underline{r},\underline{r}') = -\int_\Sigma \frac{\partial^2 G}{\partial n \partial n''} (\underline{r},\underline{r}'')G(\underline{r}'',\underline{r}')dS''$$

$$+ \int_{S_o} \frac{\partial G}{\partial n} (\underline{r},\underline{r}'') \frac{\partial G}{\partial n''} (\underline{r}'',\underline{r}')dS'', \qquad \underline{r} \in S, \quad \underline{r}' \in S. \tag{A11}$$

The kernel $L(\underline{r},\underline{r}')$ is independent of the choice of the auxiliary surface Σ as can be seen in the following way. Let S_1 be a closed surface enclosing the region V_1 and let $\underline{r}$ and $\underline{r}'$ both be either outside or inside S_1. One then has

$$\int_{S_1} \left[\nabla G(\underline{r},\underline{r}'') \frac{\partial G}{\partial n''} (\underline{r}'',\underline{r}') - \nabla \frac{\partial G}{\partial n''} (\underline{r},\underline{r}'')G(\underline{r}'',\underline{r}') \right] dS''$$

$$= \nabla \int_{S_1} \left[G(\underline{r},\underline{r}'') \frac{\partial G}{\partial n''} (\underline{r}'',\underline{r}') - G(\underline{r}'',\underline{r}') \frac{\partial G}{\partial n''} (\underline{r},\underline{r}'') \right] dS''$$

$$= \nabla \int_{V_1} \left[G(\underline{r},\underline{r}'')\nabla''^2 G(\underline{r}'',\underline{r}') - G(\underline{r}'',\underline{r}')\nabla''^2 G(\underline{r},\underline{r}'') \right] dS''$$

$$= 0. \tag{A12}$$

By letting $\underline{r}$ and $\underline{r}'$ approach points on the surface S_1 one gets

$$\int_{S_1} \left[\frac{\partial G}{\partial n}(\underline{r},\underline{r}'') \frac{\partial G}{\partial n''} (\underline{r}'',\underline{r}') - \frac{\partial^2 G}{\partial n \partial n''} (\underline{r},\underline{r}'')G(\underline{r}'',\underline{r}') \right] dS'' = 0, \qquad \underline{r} \in S_1, \quad \underline{r}' \in S_1. \tag{A13}$$

From (A13) it is then clear that $L(\underline{r},\underline{r}')$ can be cast into the following form which is explicitly independent of the auxiliary surface Σ

$$L(\underline{r},\underline{r}') = \frac{\partial}{\partial n} \int_S \frac{\partial G}{\partial n''} (\underline{r},\underline{r}'')G(\underline{r}'',\underline{r}')dS'', \qquad \underline{r} \in S, \quad \underline{r}' \in S. \tag{A14}$$

Equations (A9), (A10) and (A14) constitute a Fredholm integral equation of the second kind from which one can determine the scattered field. Before continuing with the investigation of this integral equation a corresponding integral equation of the second kind for the Neumann scattering problem will be derived.

B. Neumann Boundary Conditions

Consider the case where the open surface S is illuminated by an incident field $\psi_o(\underline{r})$. The scattered field $\psi(\underline{r})$ satisfies the Helmholtz equation (A1) outside $S + L$ and the boundary condition

$$\frac{\partial \psi^+}{\partial n} = \frac{\partial \psi^-}{\partial n} = - \frac{\partial \psi_o}{\partial n} \qquad \text{on } S. \tag{A15}$$

Using the same approach as in the case with the Dirichlet boundary conditions one arrives at the following expression

$$\frac{1}{2} \psi^+(\underline{r}) = \int_{S_o} \frac{\partial G}{\partial n''} (\underline{r},\underline{r}'') dS'' \int_S \frac{\partial G}{\partial n'} (\underline{r}'',\underline{r}') g(\underline{r}') dS'$$

$$+ \int_\Sigma \frac{\partial G}{\partial n''} (\underline{r},\underline{r}'') dS'' \int_S \frac{\partial G}{\partial n'} (\underline{r}'',\underline{r}') g(\underline{r}') dS' + \int_S G(\underline{r},\underline{r}') \frac{\partial \psi_o}{\partial n'} (\underline{r}') dS'$$

$$- \int_\Sigma G(\underline{r},\underline{r}'') dS'' \int_S \frac{\partial^2 G}{\partial n'' \partial n'} (\underline{r}'',\underline{r}') g(\underline{r}') dS' \tag{A16}$$

where

$$g(\underline{r}) = \psi^+(\underline{r}) - \psi^-(\underline{r}). \tag{A17}$$

Similarly, $\psi^-(\underline{r})$ is given by (A16) provided that one makes the following substitution in the left-hand side of (A16),

$$\psi^+(\underline{r}) \rightarrow -\psi^-(\underline{r}). \tag{A18}$$

Equations (A16)-(A18) make it possible to derive the following integral equation for $g(\underline{r})$,

$$\frac{1}{4} g(\underline{r}) - \int_S L(\underline{r}',\underline{r}) g(\underline{r}') dS' = g_o(\underline{r}) \qquad (A19)$$

where $L(\underline{r},\underline{r}')$ is given by (A14) and

$$g_o(\underline{r}) = \int_S G(\underline{r},\underline{r}') \frac{\partial \psi_o}{\partial n'} (\underline{r}') dS'. \qquad (A20)$$

Equation (A20) is the Fredholm integral equation of the second kind sought for the scattered field. The formal similarities between (A9) and (A19) is striking in that the Dirichlet and Neumann problems can be obtained from the solution of two integral equations whose kernels only differ in the order of the arguments $\underline{r}$ and $\underline{r}'$. The solutions of the two integral equations (A9) and (A19) are of course very different since the kernel $L(\underline{r},\underline{r}')$ is not symmetric.

C. Alternative Integral Equations

The solutions of the integral equations (A9) and (A19) must satisfy the edge conditions on L. A careful investigation shows that the integral operators with the kernels $L(\underline{r},\underline{r}')$ or $L(\underline{r}',\underline{r})$ does not in general transform a function satisfying certain edge conditions into a function satisfying the same edge conditions. Starting with the integral equations (A9) and (A19) alternative integral equations will be derived with kernels that preserve the edge conditions.

For that reason consider the following integral expression (the reason for doing this will become clear later on)

$$\underline{N}(\underline{r},\underline{r}') = \oint_L G(\underline{r},\underline{r}'') G(\underline{r}'',\underline{r}') d\underline{\ell}'', \qquad \underline{r},\underline{r}' \notin S+L \qquad (A21)$$

so that with $\underline{a} = \underline{a}(\underline{r})$ being an arbitrary vector satisfying necessary continuity requirements one has, by using the Stoke theorem,

$$\underline{a}\cdot[\nabla\times\underline{N}(\underline{r},\underline{r}')] = \int_S \underline{a}\cdot\nabla\times[\underline{n}''\times\nabla G(\underline{r}'',\underline{r}') G(\underline{r},\underline{r}'')] dS''$$

$$+ \int_S G(\underline{r}'',\underline{r}')\underline{a}\cdot\nabla\times[\underline{n}''\times\nabla''G(\underline{r},\underline{r}'')] dS''. \qquad (A22)$$

63

Furthermore, since $\nabla G(\underline{r},\underline{r}'') = -\nabla''G(\underline{r},\underline{r}'')$ and since $\nabla^2 G(\underline{r},\underline{r}'') - p^2 G(\underline{r},\underline{r}'') = 0$ for $\underline{r} \notin S+L$ one gets

$$\underline{a}\cdot\nabla\times[\underline{n}''\times\nabla''G(\underline{r}'',\underline{r}')G(\underline{r},\underline{r}'')] = \nabla''G(\underline{r},\underline{r}'')\cdot[\underline{a}\times(\underline{n}''\times\nabla''G(\underline{r}'',\underline{r}'))] \qquad (A23)$$

so that

$$\underline{a}\cdot\nabla\times[\underline{n}''\times\nabla''G(\underline{r},\underline{r}'')] = -p^2\underline{a}\cdot\underline{n}''G(\underline{r},\underline{r}'') - (\underline{a}\cdot\nabla)(\underline{n}''\cdot\nabla)G(\underline{r},\underline{r}''). \qquad (A24)$$

Therefore,

$$\underline{a}\cdot[\nabla\times N(\underline{r},\underline{r}')] = \int_S \{\underline{a}\times[\underline{n}''\times\nabla''G(\underline{r}'',\underline{r}')]\}\cdot\nabla''G(\underline{r},\underline{r}'')dS''$$

$$- p^2 \int_S \underline{a}\cdot\underline{n}''G(\underline{r},\underline{r}'')G(\underline{r}'',\underline{r}')dS''$$

$$- \int_S (\underline{a}\cdot\nabla)(\underline{n}''\cdot\nabla)G(\underline{r},\underline{r}'')G(\underline{r}'',\underline{r}')dS' \qquad (A25)$$

and by letting $\underline{r}$ and $\underline{r}'$ approach points on S and by putting $\underline{a}(\underline{r}) = \underline{n}(\underline{r})$, $\underline{r} \in S$ one obtains

$$\frac{\partial}{\partial n} \int_S \frac{\partial G}{\partial n''} (\underline{r},\underline{r}'')G(\underline{r}'',\underline{r}')dS'' = \int_S \{\underline{n}\times[\underline{n}''\times\nabla''G(\underline{r}'',\underline{r}')]\}\cdot\nabla''G(\underline{r},\underline{r}'')dS''$$

$$- p^2 \int_S \underline{n}\cdot\underline{n}''G(\underline{r},\underline{r}'')G(\underline{r}'',\underline{r}')dS''$$

$$- \underline{n}\cdot\nabla\times \oint_L G(\underline{r},\underline{r}'')G(\underline{r}'',\underline{r}')d\underline{\ell}'' \qquad (A26)$$

where $\int$ denotes the principal value integral.

Similarly, by making the same manipulations on the right-hand side of (A9) one arrives at the following expressions

$$\hat{f}_o(\underline{r}) = - \frac{\partial}{\partial n} \int_S \frac{\partial G}{\partial n'} (\underline{r},\underline{r}')\phi_o(\underline{r}')dS'$$

$$= - \int_S \{\underline{n}\times[\underline{n}'\times\nabla'\phi_o(\underline{r}')]\}\cdot\nabla'G(\underline{r},\underline{r}')dS' + p^2 \int_S \underline{n}\cdot\underline{n}'G(\underline{r},\underline{r}')\phi_o(\underline{r}')dS'$$

$$+ \underline{n}\cdot\nabla\times \oint_L G(\underline{r},\underline{r}')\phi_o(\underline{r}')d\underline{\ell}' \qquad\qquad (A27)$$

resulting in the following alternative equation for $f(\underline{r})$

$$\frac{1}{4} f(\underline{r}) - \int_S \hat{L}(\underline{r},\underline{r}')f(\underline{r}')dS' = \hat{f}_o(\underline{r}') + \underline{n}\cdot\nabla\times \oint_L G(\underline{r},\underline{r}')\phi_o(\underline{r}')dS'$$

$$- \underline{n}\cdot\nabla\times \int_S f(\underline{r}')dS' \oint_L G(\underline{r},\underline{r}'')G(\underline{r}'',\underline{r}')d\underline{\ell}'' \qquad (A28)$$

where

$$\hat{L}(\underline{r},\underline{r}') = \int_S \{\underline{n}\times[\underline{n}''\times\nabla''G(\underline{r}'',\underline{r}')]\}\cdot\nabla''G(\underline{r},\underline{r}'')dS''$$

$$- p^2 \int_S \underline{n}\cdot\underline{n}''G(\underline{r},\underline{r}'')G(\underline{r}'',\underline{r}')dS'' \qquad\qquad (A29)$$

and

$$\hat{f}_o(\underline{r}) = - \int_S \{\underline{n}\times[\underline{n}'\times\nabla'\phi_o(\underline{r}')]\}\cdot\nabla G(\underline{r},\underline{r}')dS'$$

$$+ p^2 \int_S \underline{n}\cdot\underline{n}'G(\underline{r},\underline{r}')\phi_o(\underline{r}')dS'. \qquad\qquad (A30)$$

The last two terms in (A28) cancel as can be seen from the following consideration.
By changing the order of integration in the last term of (A30) and observing
that $\phi(\underline{r}) = -\phi_o(\underline{r})$ on S+L one obtains

$$\underline{n}\cdot\nabla\times \oint_L G(\underline{r},\underline{r}'')d\underline{\ell}'' \int_S G(\underline{r}'',\underline{r}')f(\underline{r}')dS' = \underline{n}\cdot\nabla\times \oint_L G(\underline{r},\underline{r}'')\phi_o(\underline{r}'')d\underline{\ell}''. \qquad (A31)$$

To sum up, the following integral equation has been derived

$$\frac{1}{4} f(\underline{r}) - \int_S \hat{L}(\underline{r},\underline{r}') f(\underline{r}') dS' = \hat{f}_0(\underline{r}) \qquad (A32)$$

which is the Fredholm integral equation of the second kind sought for the scattered field. The integral equation (A32) has been used in Sec. V to formulate an equation which was used to study certain properties of the transverse magnetic field on two parallel plates of finite width.

Appendix B
Properties of the Kernel $\hat{L}_1(x,x';p)$ in (46)

This appendix presents a study of how an integral operator defined by the kernel $\hat{L}_1(x,x';p)$ transforms a function $f(x)$ of the form

$$f(x) = (w^2 - x^2)^{-\alpha} g(x) \tag{B1}$$

where $g(x)$ is continuous for $|x| \leq w$ and $g(\pm w) \neq 0$. The kernel $\hat{L}_1(x,x';p)$ is defined by

$$\hat{L}_1(x,x';p) = \frac{1}{\pi^2 (x-x')} \ln \left[\frac{(w+x)(w-x')}{(w-x)(w+x')} \right]. \tag{B2}$$

One has

$$F(x) = \int_{-w}^{w} \hat{L}_1(x,x';p) f(x') dx'$$

$$= \frac{1}{\pi^2} \int_{-w}^{w} \frac{1}{x-x'} \ln \left[\frac{(w+x)(w-x')}{(w-x)(w+x')} \right] (w^2 - x'^2)^{-\alpha} g(x') dx'$$

$$= \frac{1}{\pi^2} (w^2 - x^2)^{-\alpha} \int_0^{\infty} \left(\frac{\xi\eta+1}{\xi+1} \right)^{2\alpha-1} \frac{\ln \eta}{(\eta-1)\eta^{\alpha}} g\left(\frac{\xi\eta-1}{\xi\eta+1} \right) d\eta \tag{B3}$$

where

$$\xi = \frac{w+x}{w-x} .$$

It is easy to see that the integral in (B3) is finite for all values of x such that $|x| \leq w$. The integral therefore defines a function which is continuous and finite for $|x| \leq w$. Thus, $F(x)$ is of the form (B1), showing that any function of the form (B1) is transformed into a function of the same form by an integral operator defined by the kernel $\hat{L}_1(x,x';p)$.

Next, the values of α are found that allow nontrivial solutions of (44). Substituting the expression

$$u_{\pm}(x) = (w^2 - x^2)^{-\alpha} g_{\pm}(x), \qquad \alpha < 1 \tag{B4}$$

67

into (44) multiplying this equation by $(w^2 - x^2)^\alpha$ and putting $x = w$ in the equation thus obtained one arrives at the following expression

$$g_\pm(w)[1 - h(\alpha)] = 0 \tag{B5}$$

where

$$h(\alpha) = \frac{1}{\pi^2} \int_0^\infty \frac{\ln \eta}{(\eta-1)\eta^\alpha}\, d\eta.$$

It is easy to see that (i) $h(\alpha)$ has a minimum for $\alpha = \frac{1}{2}$ and (ii) that $h(\frac{1}{2}) = 1$. Thus, the only value of α for which (44) has a solution such that $g_\pm(\pm w) \neq 0$ is $\alpha = \frac{1}{2}$, showing that the solutions of (44) indeed satisfy the edge conditions at $x = \pm w$.

Acknowledgement

References

1. C.E. Baum, "Impedances and Field Distributions for Parallel Plate Transmission Line Simulators," Sensor and Simulation Note 21, June 1966.

2. C.E. Baum, "General Principles for the Design of ATLAS I and II, Part V: Some Approximate Figures of Merit for Comparing the Waveforms Launched by Imperfect Pulser Arrays onto TEM Transmission Lines," Sensor and Simulation Note 148, May 1972.

3. A.E.H. Love, "Some Electrostatic Distributions in Two Dimensions," Proc. London Math. Soc., Vol. 22, pp. 337-369, 1923.

4. T.L. Brown and K.D. Granzow, "A Parameter Study of Two Parallel Plate Transmission Line Simulators of EMP Sensor and Simulation Note 21," Sensor and Simulation Note 52, April 1968.

5. G.W. Carlisle, "Impedance and Fields of Two Parallel Plates of Unequal Width," Sensor and Simulation Note 90, July 1969.

6. P. Moon and D.E. Spencer, Field Theory Handbook, Springer-Verlag, Heidelberg, 1961.

7. L. Marin, "Effect of Replacing One Conducting Plate of a Parallel-Plate Transmission Line by a Grid of Rods," Sensor and Simulation Note 118, October 1970.

8. L. Marin, "Transient Electromagnetic Properties of Two Parallel Wires," Sensor and Simulation Note 173, March 1973.

9. L. Marin and R.W. Latham, "Analytical Properties of the Field Scattered by a Perfectly Conducting, Finite Body," Interaction Note 92, January 1972.

10. T. Carleman, "Über die Abelsche Integralgleichungen mit konstanten Integrationsgrenzen," Math. Zeits. Vol. 15, pp. 111-120, 1922.

11. N. Marcuvitz, Waveguide Handbook, Boston Technical Publishers, Inc., Boston, 1964.